Am J Cancer Res 2023;13(12):5846-5867
www.ajcr.us /ISSN:2156-6976/ajcr0152058

*Original Article*

# GAPDH: unveiling its impact as a key hypoxia-related player in head and neck squamous cell carcinoma tumor progression, prognosis, and therapeutic potential

Cong Peng, Huiping Ye, Zhuguang Yi

*Department of Otolaryngology, Guizhou Provincial People's Hospital, Guiyang, Guizhou, China*

Received July 5, 2023; Accepted November 1, 2023; Epub December 15, 2023; Published December 30, 2023

**Abstract:** Head and neck squamous cell carcinoma (HNSCC), characterized by hypoxia patterns, ranks as the sixth most prevalent malignant tumor worldwide. Glyceraldehyde-3-phosphate dehydrogenase (*GAPDH*) plays a role in oncogenesis under hypoxic conditions in various cancers. However, its precise function in HNSCC, especially under varied hypoxic conditions, including at high altitudes, remains unclear. Elevated *GAPDH* mRNA and protein levels in HNSCC relative to normal tissues have been demonstrated through data from The Cancer Genome Atlas (TCGA), GSE29330, and the Human Protein Atlas ($P<0.05$). This elevation was further confirmed through *in vitro* experiments utilizing two HNSCC cell lines and a normal oral mucosal epithelial cell line. Additionally, data from TCGA and GSE41613 reveal a correlation between elevated *GAPDH* expression and diminished overall and progression-free survival in patients ($P<0.05$). Subsequent analysis identifies *GAPDH* as an independent risk factor for HNSCC ($P<0.05$). Using the ESTIMATE and single-sample gene set enrichment analysis (ssGSEA) algorithms, high *GAPDH* expression was found to be associated with reduced immune scores and diminished anti-tumor cell infiltration, such as CD8+ T cells, in TCGA and GSE41613 datasets ($P<0.05$). Analysis of single-cell RNA sequencing data from GSE139324 suggests that elevated *GAPDH* expression hinders communication between plasmacytoid dendritic cells and mast cells ($P<0.05$). Furthermore, in the TCGA and GSE41613 datasets, *GAPDH*'s biological function is closely tied to hypoxia through Gene Ontology (GO), Kyoto Encyclopedia of Genes and Genomes (KEGG), and Gene Set Variation Analysis (GSVA) analyses. Moreover, its expression is linked to one cuproptosis-related gene, five N6-methyladenosine-related genes, six immune checkpoint genes, and pivotal pathways such as *MYC* and *E2F* ($P<0.05$). *GAPDH* showed excellent predictive value in estimating the efficacy of immunotherapy and 11 anti-tumor drugs (e.g., cisplatin) ($P<0.05$), using TIDE and pRRophetic algorithms on the TCGA and GSE41613 datasets. Under 1% $O_2$ *in vitro*, HNSCC cells show elevated *GAPDH* expression, leading to decreased apoptosis and increased migration, clonogenicity, invasiveness, and resistance to cisplatin ($P<0.05$). At 5% $O_2$, these effects persisted, albeit less pronouncedly. Inhibiting *GAPDH* reversed these effects under all oxygen concentrations ($P<0.05$). Overall, our findings reveal *GAPDH* as a key hypoxia-related player influencing tumor progression, prognosis, and therapeutic potential in HNSCC.

**Keywords:** Hypoxia, head and neck squamous cell carcinoma, immunotherapy, cisplatin, *GAPDH*

## Introduction

Head and neck squamous cell carcinoma (HNSCC) is a highly prevalent and aggressive malignancy that is derived from the transformation of squamous cells lining the mucosal surfaces of the head and neck region. In 2020, HNSCC accounted for 3.8% (744,944/19,300,000) of the newly diagnosed cancer cases and 3.6% (364,339/10,000,000) of the cancer-related deaths [1]. In Europe, the total healthcare expenses for HNSCC reached up to 665 million euros, with an average individual cost of £23,212 [2, 3]. Despite these significant investments, the 5-year survival rate for HNSCC remains below 50% due to factors such as tumor recurrence and metastasis, along with resistance to radiotherapy, chemotherapy, and limited immunotherapy efficacy [4, 5]. This underscores the urgency to uncover the molec-

ular mechanisms driving HNSCC progression and treatment resistance.

Hypoxia is a characteristic feature of solid tumors, including HNSCC, and plays a significant role in promoting tumor progression, therapy resistance, and metastasis [6]. The association between hypoxia and tumor development is evident in high-altitude regions, where oxygen levels, typically 20%-40% lower than at sea level, induce hypoxia in the human body [7]. Studies in these regions have underscored the impact of hypoxia on tumor characteristics. For example, breast cancer patients in high-altitude areas, like Tibet, often present with larger tumors and more advanced clinical pathological features [8]. Conversely, gastric adenocarcinoma patients in low-altitude regions tend to have notably better prognoses than those in high-altitude areas [9]. Additionally, individuals living above 2000 meters in altitude experience an increased risk of developing various cancers, including gastric, colorectal, hepatobiliary, breast, and lymphohematopoietic malignancies, and a correspondingly higher mortality risk from these diseases [10]. These findings collectively emphasize the intricate link between hypoxia and tumor development, as well as their impact on clinical outcomes.

Despite the known importance of hypoxia in tumor progression, research into the crucial regulatory genes influencing HNSCC in hypoxic environments, especially in varied hypoxic conditions such as those in high-altitude regions, remains sparse. While a predictive scoring system comprising 49 hypoxia-related genes has been developed for HNSCC [11], a thorough understanding of the specific functionalities of these genes within hypoxic settings is still lacking. One such gene, Glyceraldehyde-3-phosphate dehydrogenase (*GAPDH*), traditionally known as a housekeeping gene and a key glycolytic enzyme, has recently emerged as a focal point in cancer research due to its diverse roles [12-19]. Numerous studies have reported elevated *GAPDH* expression under hypoxic conditions across varied cell types and organs [20-23]. Furthermore, potential *GAPDH* instability has been observed in blood samples from high-altitude regions [24, 25], and even short-term moderate hypoxia, like during air travel, can boost *GAPDH* protein levels in human serum [26]. *GAPDH* also plays a pivotal role in enhancing tumor invasiveness and resistance to treatment under hypoxic circumstances, as observed in hepatocellular carcinoma [27] and malignant leukemia [28]. A particular study even highlighted elevated mRNA expression levels of *GAPDH* in the plasma of untreated HNSCC patients in comparison to healthy individuals [29]. However, the precise roles of *GAPDH* in HNSCC, particularly under mild to severe hypoxic conditions, and its therapeutic implications remain to be fully elucidated.

Therefore, in this study, using the Cancer Genome Atlas (TCGA) and the Gene Expression Omnibus (GEO) datasets, we explored *GAPDH* expression disparities between HNSCC and normal tissues and investigated its correlation with patient survival. Employing single-cell RNA sequencing data (scRNA-seq) and single-sample gene set enrichment analysis (ssGSEA), we assessed the relationship between *GAPDH* expression and the tumor immune microenvironment (TIME). Using Tumor Immune Dysfunction and Exclusion (TIDE), the Cancer Immunome Atlas (TCIA), and pRRophetic algorithms, we explored the link between *GAPDH* levels in HNSCC and response efficacy to immunotherapy and antitumor drugs. Through *in vitro* experiments, we explored the impact of *GAPDH* expression variations on cell behavior and cisplatin sensitivity in HNSCC cell lines under 1%, 5%, and 21% oxygen concentrations. This study aims to shed light on *GAPDH*'s function in HNSCC progression and its feasibility as a treatment target under varying hypoxia conditions.

## Materials and methods

### *Data collection and processing*

This study first enrolled 503 HNSCC samples and 44 normal head and neck tissue samples (n = 547). The raw RNA sequencing (RNA-seq) data expression matrices and survival information for the HNSCC cases were obtained from the TCGA database (https://portal.gdc.cancer.gov/; accessed on February 19, 2023). The general clinical information for the 503 patients was extracted from the UCSC Xena database (http://xenabrowser.net/datapages/; accessed on February 19, 2023). Then, data for HNSCC cases with a survival time of less than 30 days was excluded. Finally, we included data from 500 HNSCC patients for subsequent analyses (Supplementary Table 1). Furthermore, we

acquired RNA data expression matrices and survival information for 97 HNSCC patients in the GSE41613 dataset (Supplementary Table 2) and an additional dataset, GSE29330, which included 13 HNSCC samples and 5 normal tissue samples for further analysis. Both datasets were sourced from the GEO database (http://www.ncbi.nlm.nih.gov/geo/; accessed on February 19, 2023). Moreover, scRNA-seq was extracted from the GSE139324 dataset, which included five tonsil tissues, thirty-one peripheral blood mononuclear cells, and 26 tumor-infiltrating lymphocytes from the five healthy donors and 26 HNSCC patients (http://www.ncbi.nlm.nih.gov/geo/; accessed on February 19, 2023) (Supplementary Table 3). The "harmony" (version: 0.1.0) and the "Seurat" R (version: 4.1.1) packages were used sequentially for removing the batch effects and normalizing the scRNA-seq data. Refer to **Figure 1** for a schematic representation of our work.

*Biological function analysis*

In both the TCGA and GSE41613 gene expression matrices, genes correlating with *GAPDH* expression were identified using a threshold of |cor|>0.6 and $P<0.001$. Subsequently, gene ontology (GO) and Kyoto Encyclopedia of Genes and Genomes (KEGG) functional analyses were performed to determine the potential biological functions and pathways associated with these correlated genes. Using the "GSVA" R package (version: 1.44.0), we further explored the functional characteristics of the biological processes between groups with different *GAPDH* expression levels in the TCGA and GSE41613 datasets. Additionally, we analyzed the functional attributes of the plasmacytoid dendritic cells (pDC) within the scRNA-seq data.

*Immune analysis and gene expression*

The tumor immune cell infiltration status and immune function in the high and low-*GAPDH* expression groups were compared using the single-sample GSEA (ssGSEA) algorithms. Concurrently, differences in the expression levels of ten cuproptosis-related genes, twenty-three the N6-methyladenosine (m6A)-related genes, and forty-seven immune checkpoint genes were analyzed between these two groups, with these genes respectively sourced from previous literature [11, 30]. TCIA (https://tcia.at/; accessed on February 20, 2023) and TIDE (http://tide.dfci.harvard.edu/; accessed on February 20, 2023) algorithms were used to predict the effects of immunotherapy in the high and low-*GAPDH* expression groups of HNSCC patients. Furthermore, the "pRRophetic" package (version: 0.5) was used to predict the responses of all the HNSCC samples in the TCGA and GSE41613 datasets to different drugs.

*Cell culture*

The FaDu and Tu212 HNSCC cell lines and the normal human oral keratinocyte (NHOK) cell line were purchased from the American Type Culture Collection (ATCC, Manassas, Virginia, USA) and cultured in a humidified incubator with Roswell Park Memorial Institute (RPMI) 1640 (Servicebio, Wuhan, China) supplemented with 10% fetal bovine serum (Chuan Qiu Biotechnology, Shanghai, China) and 1% penicillin at 37°C and 5% $CO_2$. Before exposure to the hypoxic environment, the cells were cultured for 24 hours in a medium without the serum. Cells were cultured under three different oxygen concentrations: 21% oxygen, 5% oxygen, and 1% oxygen. Additionally, to regulate the oxygen concentration, a mixed gas (5% $CO_2$, balanced with nitrogen) was infused into the sealed cell incubator, and the cells were cultured under these conditions for 4 hours. The cell lines were transfected with negative control (NC)-*GAPDH* and *GAPDH*-silenced (si-*GAPDH*) using Lipo8000™ (Beyotime, Shanghai, China). Cisplatin was purchased from Qilu Pharmaceutical Co., Ltd. (Jinan, Shandong, China).

*Quantitative reverse-transcription polymerase chain reaction and western blotting*

The qPCR assays were performed as previously described [31]. Cells' total RNA was purified using the RNA-Quick Purification Kit (NCM Biotech, Suzhou, China). Subsequent quantification was performed in triplicate through qRT-PCR on a Bio-Rad CFX96, utilizing the SYBR Green method (Takara, Mountain View, CA, USA). Supplementary Table 4 contains the corresponding primer sequences.

Western blot (WB) was performed according to standard protocol [31]. Total cellular protein extracts (Shanghai Epizyme Biomedical Technology Co., Ltd., Shanghai, China) were pre-

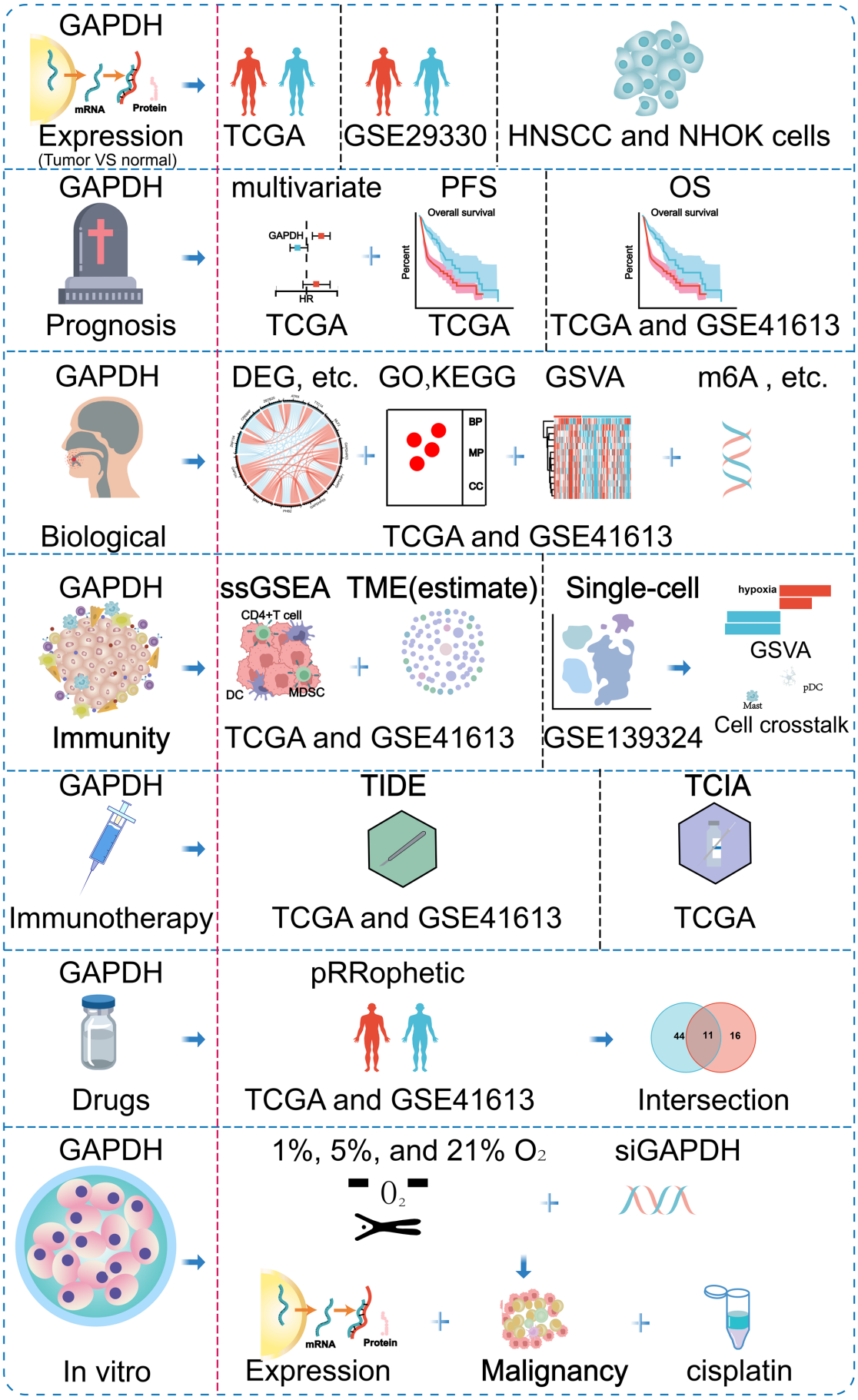
GAPDH
mRNA
Protein
Expression
(Tumor VS normal)
TCGA
GSE29330
HNSCC and NHOK cells
GAPDH
Prognosis
multivariate
GAPDH
HR
TCGA
PFS
Overall survival
Percent
TCGA
OS
Overall survival
Percent
TCGA and GSE41613
GAPDH
Biological
DEG, etc.
GO,KEGG
BP
MP
CC
GSVA
m6A , etc.
TCGA and GSE41613
GAPDH
Immunity
ssGSEA
CD4+T cell
DC
MDSC
TME(estimate)
TCGA and GSE41613
Single-cell
GSE139324
hypoxia
GSVA
pDC
Mast
Cell crosstalk
GAPDH
Immunotherapy
TIDE
TCGA and GSE41613
TCIA
TCGA
GAPDH
Drugs
pRRophetic
TCGA and GSE41613
44
11
16
Intersection
GAPDH
In vitro
1%, 5%, and 21% O2
O2
siGAPDH
mRNA
Protein
Expression
Malignancy
cisplatin

**Figure 1.** Flow chart of this study. Note: TCGA, The Cancer Genome Atlas; OS, overall survival; PFS, progression-free survival; DEG, Differentially Expressed Genes; GO, Gene Ontology; KEGG, Kyoto Encyclopedia of Genes and Genomes; GSVA, Gene Set Variation Analysis; m6A, N6-Methyladenosine; ssGSEA, Single-sample Gene Set Enrichment Analysis; TME, Tumor Microenvironment; TIDE, Tumor Immune Dysfunction and Exclusion; TCIA, The Cancer Immunome Atlas.

pared from different cell samples and quantified. Then, equal amounts of proteins were separated by gel electrophoresis and transferred onto a PVDF membrane. Then, the membranes were blocked by incubation with skimmed milk for 1 hour. Then, the blots were incubated with the primary *GAPDH* Polyclonal antibody or Beta Actin Recombinant antibody (Proteintech, Wuhan, China) overnight at 4°C. Subsequently, after washing, the membrane was incubated with the HRP-conjugated Affinipure Goat Anti-Rabbit IgG (H+L) (Proteintech, Wuhan, China) conjugated to a reporter enzyme. The membranes were developed using the appropriate detection system and the bands corresponding to *GAPDH* were quantified in the samples.

*Apoptosis assay*

FaDu and TU212 cells were seeded in 6-well plates. Twenty-four hours post-transfection, cells were collected and stained using Annexin V-FITC and propidium iodide (PI) solutions (BD Biosciences, San Jose, CA, USA). Flow cytometric data were subsequently processed using BD FACSDiva software V6.1.3 (BD Biosciences).

*CCK-8 assay*

The cell growth and survival rates were measured using the Cell Counting Kit-8 (CCK-8) (Beyotime, Shanghai, China). Briefly, $2\times10^3$ cells per well were seeded in the 96-well plates (Servicebio, Wuhan, China) and cultured for 48 hours. Then, 10 μl of CCK-8 reagent was added to each well and the cells were further incubated at 37°C for 1 hour. The optical density of each well was measured at 450 nm at 24 hours.

*Scratch assay*

FaDu and TU212 cells in their exponential growth phase were trypsinized and seeded at a density of $5\times10^5$ cells per well in six-well plates containing DMEM. Once the cells adhered after approximately 12 hours, a sterile 1 ml pipette tip was utilized to create a linear scratch in the center of each well. Detached cells were gently washed away using phosphate-buffered saline. The wells were then replenished with fresh DMEM supplemented with 2% FBS and incubated at 37°C. The migration of the cells into the scratch was observed at 0 and 24 hours using phase contrast on an inverted microscope. For quantification, the unhealed area of the scratch was measured using ImageJ software.

*Transwell migration assays*

Transwell migration assays were performed according to previously published protocols [32]. Briefly, cells in culture medium without serum were added into the upper chamber of the Transwell (Corning, USA) and medium with serum was added into the lower chamber. The Transwell chambers are then incubated for 24 hours. After incubation, non-migrated cells in the upper chamber are gently removed with a cotton swab. Migrated cells on the lower side of the membrane are fixed with a solution like 4% paraformaldehyde. Fixed cells are then stained with a dye such as 0.1% crystal violet. Finally, the images were captured under a light microscope (×200 magnification) (Nikon, Japan).

*Colony formation assay*

The logarithmically growing cells were detached from culture dishes using 0.25% trypsin. The cell density was adjusted to 250 cells/ml. The cells were then incubated in a six-well plate at 37°C and 5% $CO_2$ over a 2-3-week period. The medium was replaced thrice a week. Then, the cells were harvested, fixed with methanol, and stained for 30 minutes with 1 ml of Giemsa solution per well. Then, after rinsing thoroughly in water, the colonies were counted under a light microscope (Nikon, Japan).

*Statistical analysis*

Statistical analysis was performed using the R software (version: 4.2.0). Kaplan-Meier survival curves and log-rank tests were used to assess

the differences in survival rates between different subgroups of HNSCC patients. Univariate and multivariate Cox regression analyses were performed to determine if *GAPDH* expression was an independent prognostic factor in patients with HNSCC. The statistical differences between the high- and low-*GAPDH* expression groups were analyzed using the Wilcoxon test. The statistical differences between multiple groups were analyzed using the Kruskal-Wallis test. Spearman test was used for the correlation analysis. The *in vitro* experiments were performed at least three times. The data was plotted using the GraphPad Prism software (version: 9.0). Continuous variables conforming to a normal distribution were represented as mean ± standard deviation. The independent t-test was used for a pairwise comparison of data between two groups. One-way analysis of variance was used for comparing data from multiple groups. $P<0.05$ was considered statistically significant.

## Results

### *GAPDH is aberrantly overexpressed in HNSCC*

A panel of 49 hypoxia-related genes by univariate (Supplementary Figure 1A) and multivariate Cox regression analyses (Supplementary Figure 1B) and *PGK1*, *P4HA1*, *MCTS1*, *GAPDH*, *ENO1*, and *CORO1C* were identified as independent prognostic factors that were associated with the overall survival (OS) of patients with HNSCC in the TCGA database. Previous studies have demonstrated the roles of *PGK1* [33], *P4HA1* [34], *MCTS1* [35], *ENO1* [36], and *CORO1C* [37] in HNSCC, but the role of *GAPDH* in HNSCC is not well established. TIMER2.0 database (http://timer.cistrome.org/) analyses was used to evaluate the expression levels of *GAPDH* in the several tumors and their corresponding normal tissue samples. In most cancer types, including HNSCC, *GAPDH* levels were significantly higher in the tumor tissues compared to the corresponding normal tissues (Supplementary Figure 1C). The only exception was prostate adenocarcinoma, in which *GAPDH* expression levels did not show significant differences between the tumor and the corresponding normal tissue samples. Subsequently, in both TCGA (**Figure 2A**, **2B**) and GSE29330 (**Figure 2C**) datasets, *GAPDH* expression was found to be significantly elevated in HNSCC tissues compared to normal tissues ($P<0.05$). To validate our findings, we analyzed *GAPDH* protein expression in HNSCC tissues using the HPA database (https://www.proteinatlas.org/), where immunohistochemical staining revealed a moderate staining intensity for *GAPDH* in HNSCC tissues and a weaker intensity in the normal tissues (**Figure 2D**). Concurrently, qPCR and WB analyses indicated markedly elevated *GAPDH* mRNA and protein expression levels in the TU212 and FaDu cell lines compared to the NHOK cells ($P<0.05$) (**Figure 2E**). Following our discovery of *GAPDH* overexpression in HNSCC tissues, we further investigated its differential expression in various HNSCC patient subgroups. Our analyses revealed no significant variation in *GAPDH* levels when comparing age groups (≤60 years vs. >60 years) or between genders (**Figure 2F**, **2G**). Intriguingly, *GAPDH* expression levels were significantly higher in patients belonging to advanced WHO grades 2-4 and TNM stages II-IV compared to those belonging to WHO grade 1 and TNM stage I, respectively (all $P<0.05$) (**Figure 2H**, **2I**). Tumors in advanced stages generally indicate a higher degree of malignancy. Research has shown that tumors in advanced stages tend to have elevated levels of Hypoxia-inducible factor-1alpha (HIF-1α), reflecting a pronounced hypoxic condition [38]. This might hint at a potential relationship between *GAPDH* and hypoxia in HNSCC. Our findings underscore *GAPDH*'s oncogenic role in HNSCC. They also suggest a potential association with the disease's hypoxic conditions.

### *GAPDH is an independent prognostic marker in HNSCC*

Next, we analyzed the prognostic role of *GAPDH* in HNSCC using the TCGA dataset (n = 500) and the GSE41613 dataset (n = 97) of HNSCC patients. Our results demonstrated that HNSCC patients with higher *GAPDH* expression levels were associated with shorter overall survival (OS) in both the TCGA and GSE41613 datasets (**Figure 3A**, **3C**). Furthermore, HNSCC patients with higher *GAPDH* expression levels were associated with shorter progression-free survival (PFS) (**Figure 3B**). Moreover, univariate and multivariate Cox regression analyses demonstrated that *GAPDH* was an independent prognostic factor for HNSCC (HR = 1.400, 95% CI, 1.075-1.824, $P = 0.013$) after adjusting for

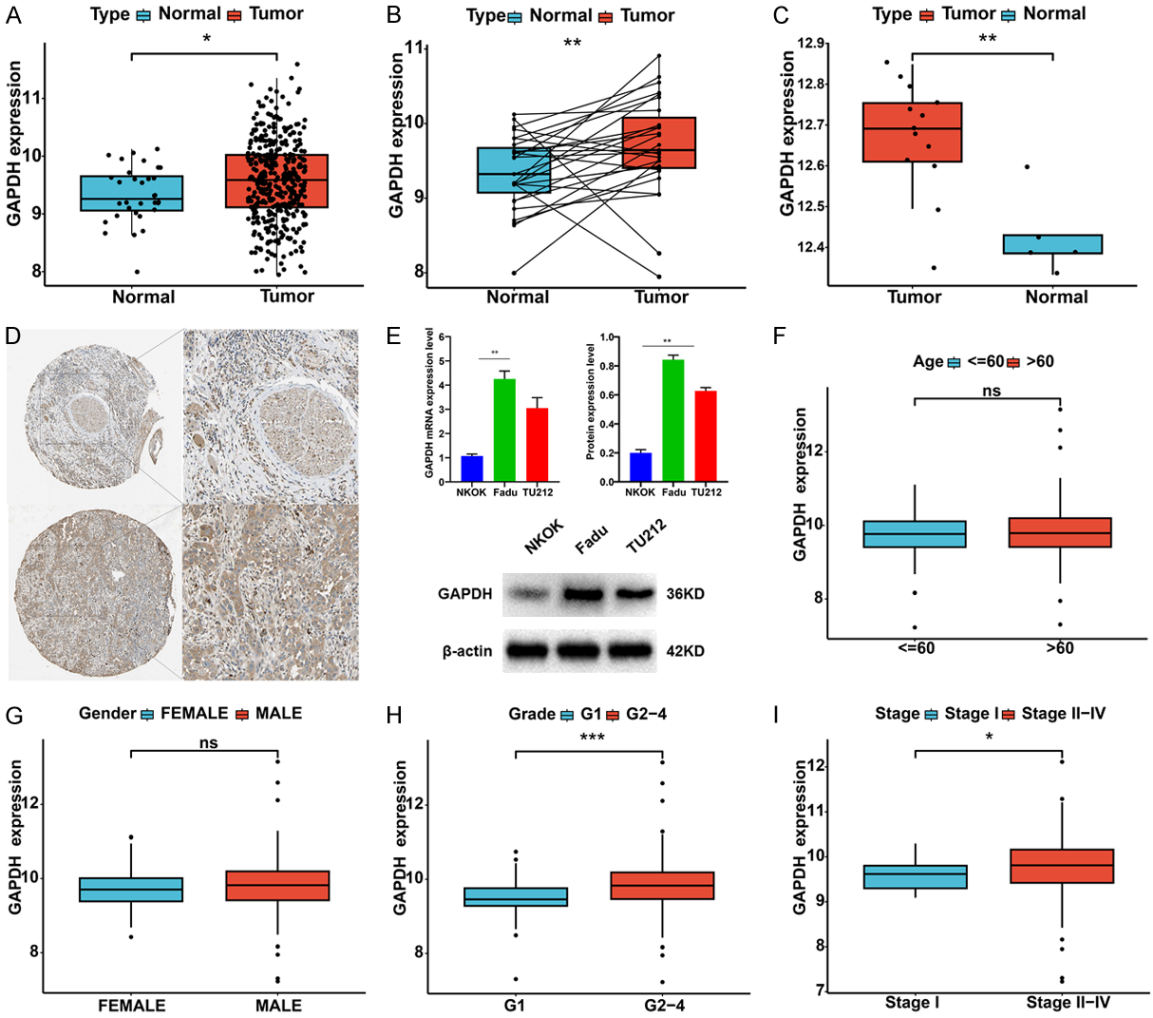


**Figure 2.** Comparative analysis of *GAPDH* mRNA and protein expression in HNSCC tissues and normal head and neck tissue samples. (A, B) *GAPDH* mRNA expression in HNSCC versus normal tissues in TCGA: Wilcoxon rank sum test (A) and paired differentiation analysis (B). (C) Wilcoxon rank sum test analysis of *GAPDH* expression in HNSCC versus normal tissues in GSE29330. (D) Immunohistochemical staining data in the HPA database shows the expression levels of *GAPDH* protein in the HNSCC and normal head and neck tissue samples. (E) Quantitative PCR and western blot analyses results show the *GAPDH* mRNA and protein expression levels in the Tu212 and FaDu HNSCC cell lines and the normal oral mucosal NHOK cells. (F, G) *GAPDH* expression levels in HNSCC patients were stratified by age (≤60 years vs. >60 years) and gender (males vs. females). (H, I) *GAPDH* expression levels in HNSCC patients are stratified according to WHO grades (WHO grades G2-4 vs. WHO grade G1) and TNM stages (TNM stages II-IV vs. TNM stage I). Note: HPA, Human Protein Atlas; WHO, World Health Organization; TNM, tumor node metastasis. ns, $P>0.05$, $*P<0.05$, $**P<0.01$, and $***P<0.001$.

age, gender, WHO grades, and TNM stages (**Figure 3D**). Since clinical characteristics are heterogeneous among tumor patients, stratified analysis is necessary to validate the prognostic value of the clinical features. Our results demonstrated that the *GAPDH* expression levels were associated with the OS of patients aged >60 years, females, WHO grades G1-2, TNM stages II-IV, closed margin status, lymph node neck dissection, no radiation therapy, radiation therapy, and smoking (**Figure 4A-I**). These results confirmed that *GAPDH* was an independent prognostic risk factor for HNSCC patients and potentially played a significant role in disease progression.

### *GAPDH expression correlates with hypoxia-associated genes and pathways in HNSCC*

To identify the mechanistic details underlying the oncogenic role of *GAPDH* in HNSCC, we conducted a comprehensive analysis using

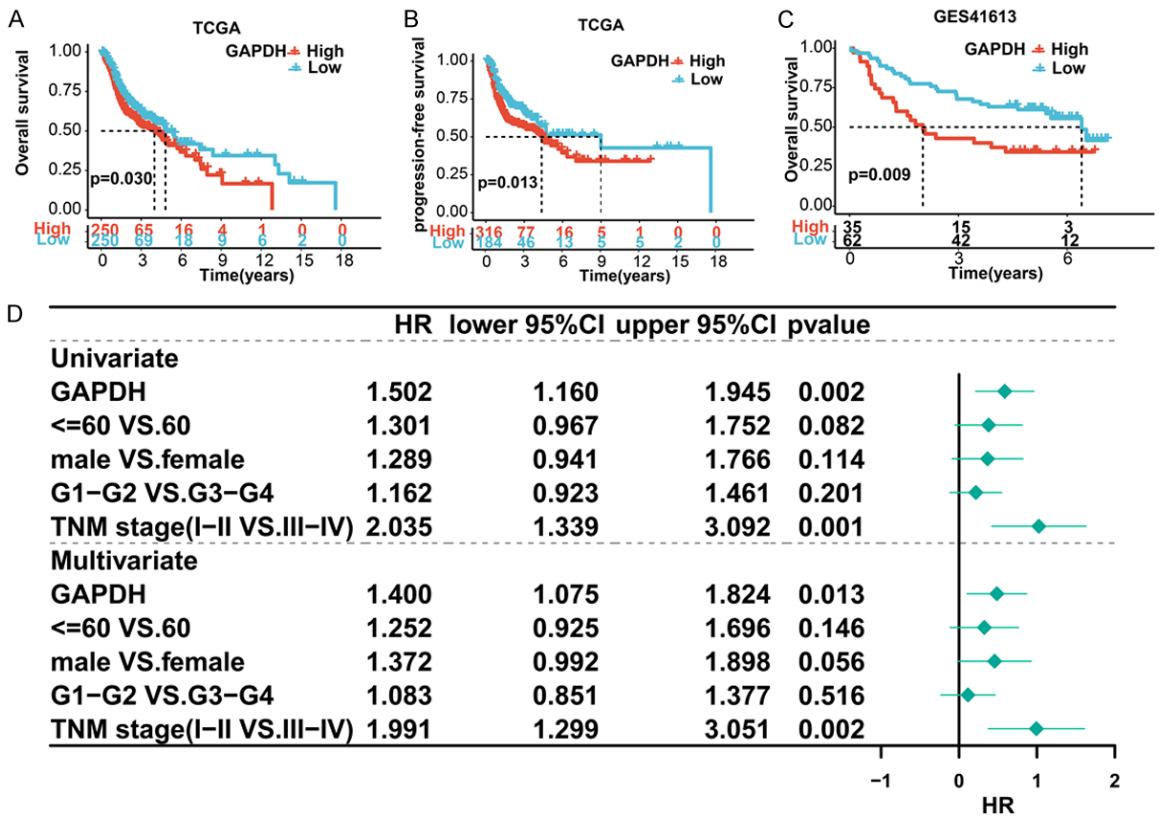


**Figure 3.** Prognostic analysis of HNSCC patients based on the *GAPDH* expression levels. A. OS of HNSCC patients in the TCGA dataset with high and low *GAPDH* expression levels. B. PFS of HNSCC patients in the TCGA dataset with high and low *GAPDH* expression levels. C. OS of HNSCC patients in the GSE41613 dataset with high and low *GAPDH* expression levels. D. Univariate and multivariate Cox regression analysis to evaluate independent prognostic value of *GAPDH* in TCGA dataset. Note: TCGA, The Cancer Genome Atlas; OS, overall survival; PFS, progression-free survival.

gene expression matrices from both TCGA and GEO datasets. Initially, as evidenced by heatmaps, genes associated with hypoxia, such as *LDHA*, *MIF*, and *CHCHD2* (as identified in previous literature [11]), were found to be upregulated in the high-*GAPDH* expression group across both TCGA and GEO datasets (**Figure 5A**). Further correlation analyses highlighted genes such as *MLF2*, *PHB2,* and *AQP1*, previously reported to regulate tumorigenesis through hypoxia-related pathways [39-41], as being correlated with *GAPDH* (**Figure 5B**). Subsequently, GO and KEGG enrichment analyses of these *GAPDH*-correlated genes revealed significant enrichment in hypoxia-associated pathways, including glycolytic processes, ADP metabolic processes, glycolysis/gluconeogenesis, and DNA replication (**Figure 5C**, **5D**). GSVA analysis further showcased the activation of hypoxia-related pathways, such as glycolysis/gluconeogenesis and glyoxylate and dicarboxylate metabolism, as well as tumor-related pathways like the cell cycle, predominantly in the high-*GAPDH* expression group (**Figure 5E**). Overall, these findings demonstrated a close relationship between *GAPDH* expression and hypoxia in HNSCC.

*GAPDH expression and its association with the tumor immune microenvironment and potential therapeutic targets in HNSCC*

Next, the status of TIME was analyzed in the HNSCC patients with high and low-*GAPDH* expression levels. We first analyzed the status of the tumor immune environment using the ESTIMATE algorithm. In both the TCGA and GEO databases, the immune scores and estimate scores of HNSCC patients with high *GAPDH* expression were significantly lower than those with low-*GAPDH* expression ($P<0.05$) (**Figure 6A**). Considering the importance of cuproptosis and m6A in tumor progression, we analyzed genes associated with each to *GAPDH*. For

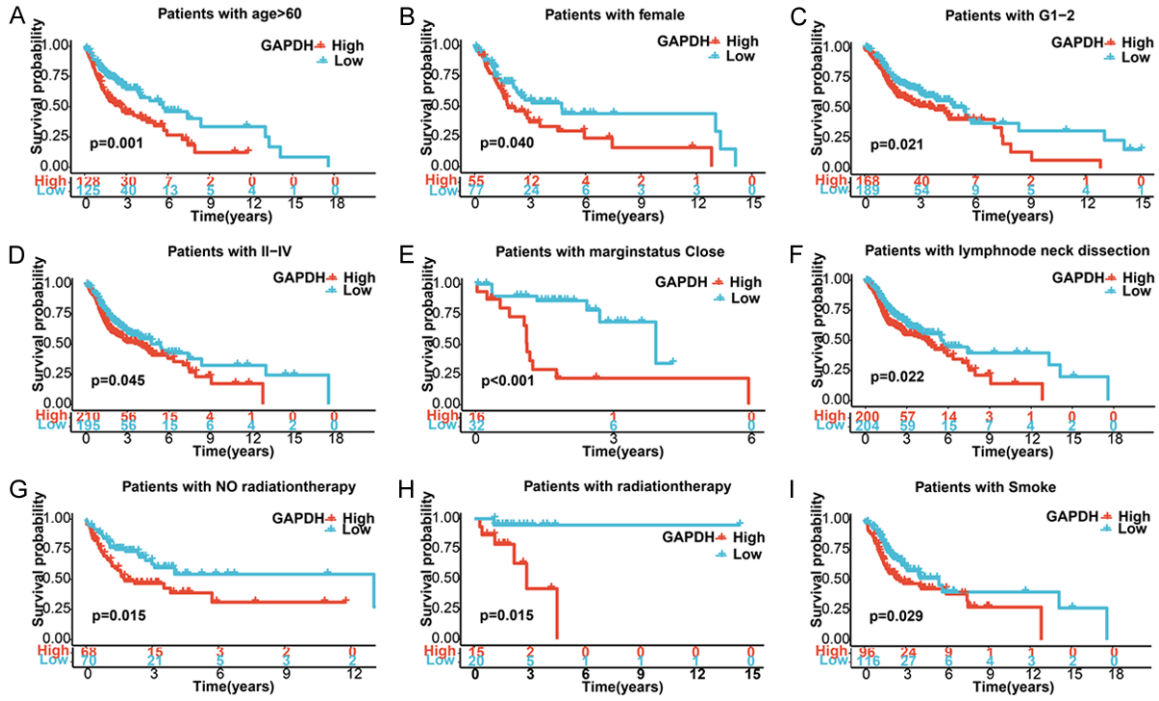


**Figure 4.** Prognostic analysis of HNSCC patients based on *GAPDH* expression levels and stratification of clinical features. (A-I) OS of HNSCC patients stratified according to *GAPDH* expression levels and clinical features, including (A) Age: >60 years; (B) Gender: female; (C) WHO grades: G1-2; (D) TNM stages: II-IV; (E) Margin status: close; (F) Lymph node neck dissection; (G) No radiation therapy; (H) Radiation therapy; and (I) Smoking: yes.

cuproptosis, *MTF1* was significantly upregulated in the high *GAPDH* expression group across these datasets ($P<0.05$) (**Figure 6B**). Similarly, m6A-related genes such as *METTL3*, *RBM15*, *HNRNPC*, *HNRNPA2B1*, and *ALKBH5* were upregulated in HNSCC patients with higher *GAPDH* expression ($P<0.05$) (**Figure 6C**). Furthermore, in light of the prominent role of immune checkpoint inhibitors in cancer therapy, we analyzed the relationship between immune checkpoint genes and *GAPDH* in HNSCC. As shown in **Figure 6D**, genes like *IDO2*, *CD276*, *HHLA2*, *CD244*, *BTLA*, and *CD40LGD* all exhibited significant differences between varying *GAPDH* expression groups ($P<0.05$). ssGSEA analysis revealed that key pathways such as *MYC* and *E2F* correlated positively with *GAPDH* expression ($P<0.05$) (**Figure 7A**). Immune function-related analysis indicated that T cell co-stimulation and type II IFN response were more active in the *GAPDH* low-expression group ($P<0.05$) (**Figure 7B**). Additionally, *GAPDH* expression correlated positively with neutrophil infiltration but negatively with the infiltration of anti-tumor CD8 T cells ($P<0.05$) (**Figure 7C**). Overall, these findings strongly suggest a close association between *GAPDH* and the immunosuppressive environment of HNSCC, offering potential therapeutic targets for its treatment.

*Validation of the role of GAPDH in HNSCC via single-cell RNA sequencing analysis*

We then performed scRNA-seq analyses to identify different subtypes of immune cells expressing *GAPDH* in the TIME. We assessed 121,347 cells from 62 samples, including according to the expression of marker genes reported in a previous study [11], and identified ten different subtypes of immune cells (**Figure 8A**). The expression levels of *GAPDH* in the ten different subtypes of immune cells are shown in **Figure 8B**. Furthermore, we observed differential expression of *GAPDH* in nine out of the ten subtypes of immune cells between HNSCC tumor and normal tissues (all $P<0.05$) (**Figure 8C**). *GAPDH* expression levels in the mast cells did not vary significantly between the HNSCC and normal tissues. pDC showed the highest expression of *GAPDH* in the HNSCC tissues (**Figure 8D**). GSVA of scRNA-seq data from the pDCs demonstrated activation of hypoxia (**Figure 8E**). To delve deeper into the role of

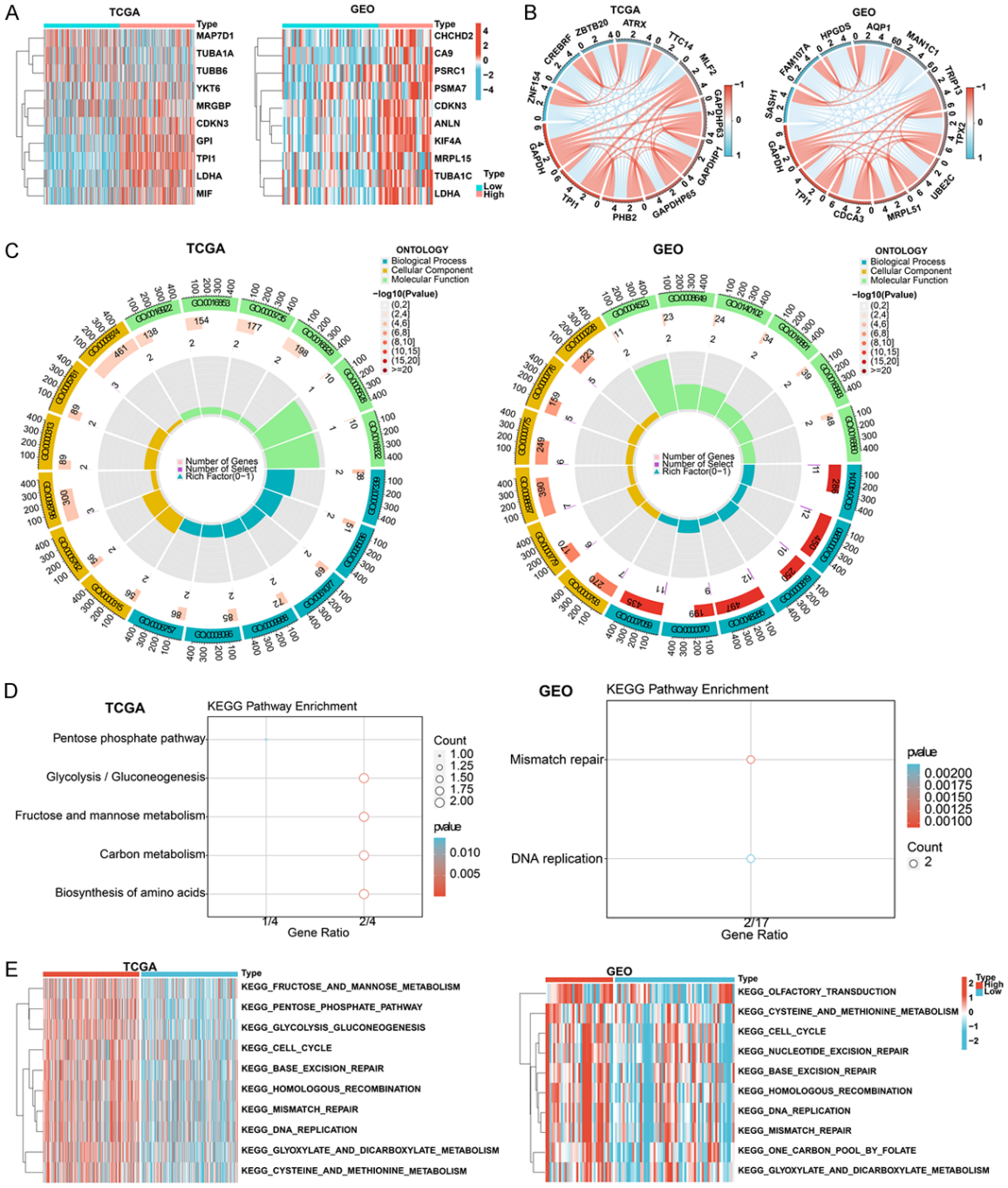


**Figure 5.** Differential Gene Expression, spearman correlation analysis, functional enrichment analysis, and GSVA of *GAPDH* and related genes in HNSCC. (A) Heatmaps displaying gene expression patterns between high- and low-*GAPDH* expressing HNSCC samples in both TCGA (left) and GSE41613 (right) databases. (B) Spearman correlation analysis shows genes that are significantly associated with *GAPDH* in TCGA (left) and GSE41613 (right) based on the gene count matrix. (C, D) GO enrichment (C) and KEGG pathway (D) analyses for genes with a correlation coefficient >0.6 with *GAPDH* in both TCGA (left) and GSE41613 (right) databases. (E) Analysis of the activation status of biological behaviors in high- and low-*GAPDH* expressing groups across TCGA (left) and GSE41613 (right) databases. Note: GSVA, gene set variation analysis; GO, Gene Ontology; KEGG, Kyoto Encyclopedia of Genes and Genomes.

*GAPDH* in TIME, we categorized pDCs into high and low *GAPDH* expression groups and further analyzed them using the 'cellchat' R package (version: 1.5.0). Compared to pDCs with high *GAPDH* expression, those with lower expression showed enhanced communication with

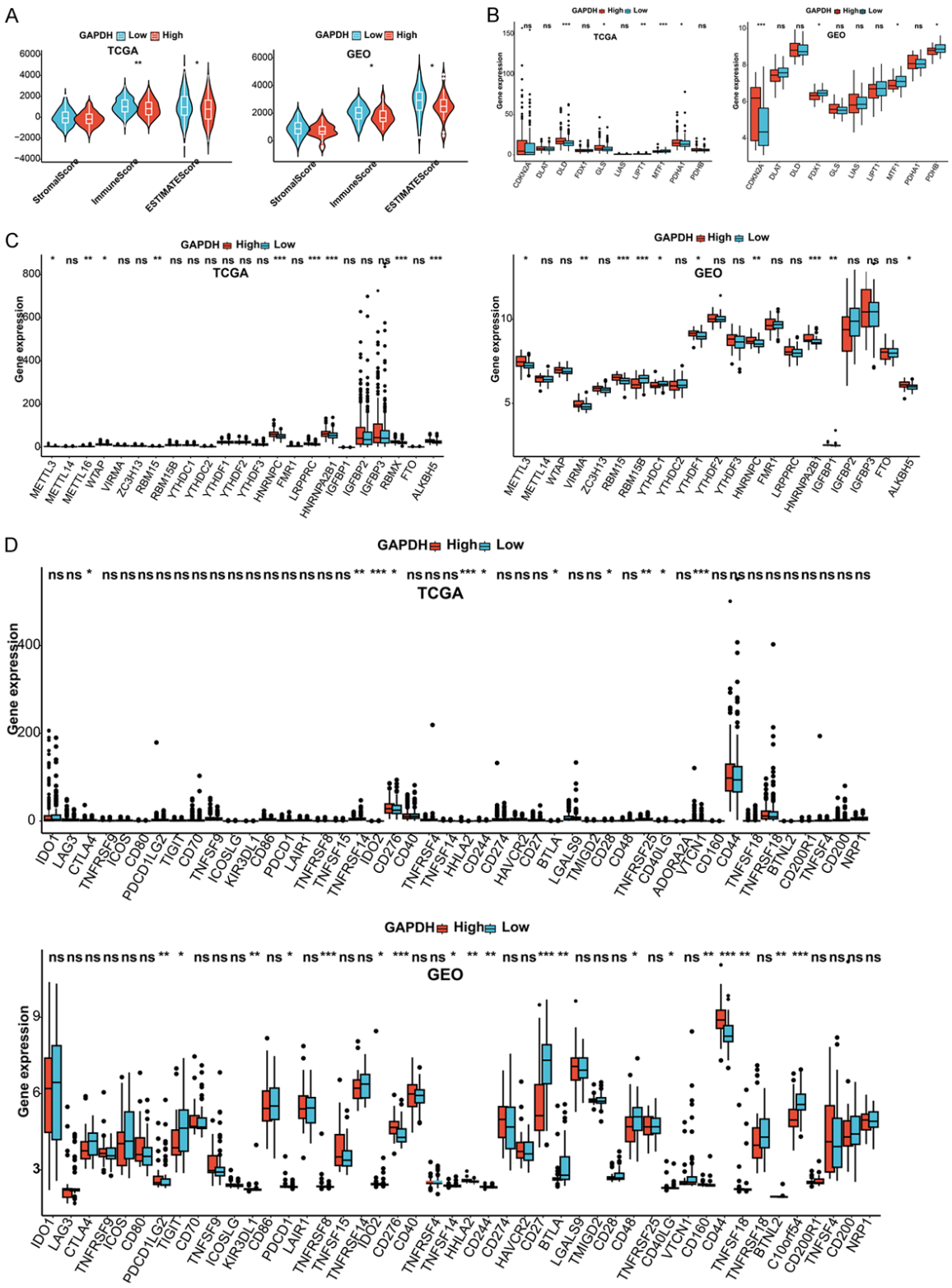


**Figure 6.** Correlation analysis between *GAPDH* expression levels in the HNSCC tissues and the status of the tumor immune microenvironment and the expression levels of cuproptosis-, m6A-related, and the immune checkpoint genes. (A) ESTIMATE algorithm shows the immune scores and estimate scores of HNSCC patients with high- and low-*GAPDH* expression in TCGA (left) and GSE41613 (right) datasets. (B-D) Comparative analysis of the expression levels of several cuproptosis-related genes (B), m6A-related genes (C), and immune checkpoint genes (D) between HNSCC tumors with high and low *GAPDH* expression in TCGA (left or top) and GSE41613 (right or bottom). Note: ns, $P>0.05$, ***$P<0.001$, **$P<0.01$, *$P<0.05$.

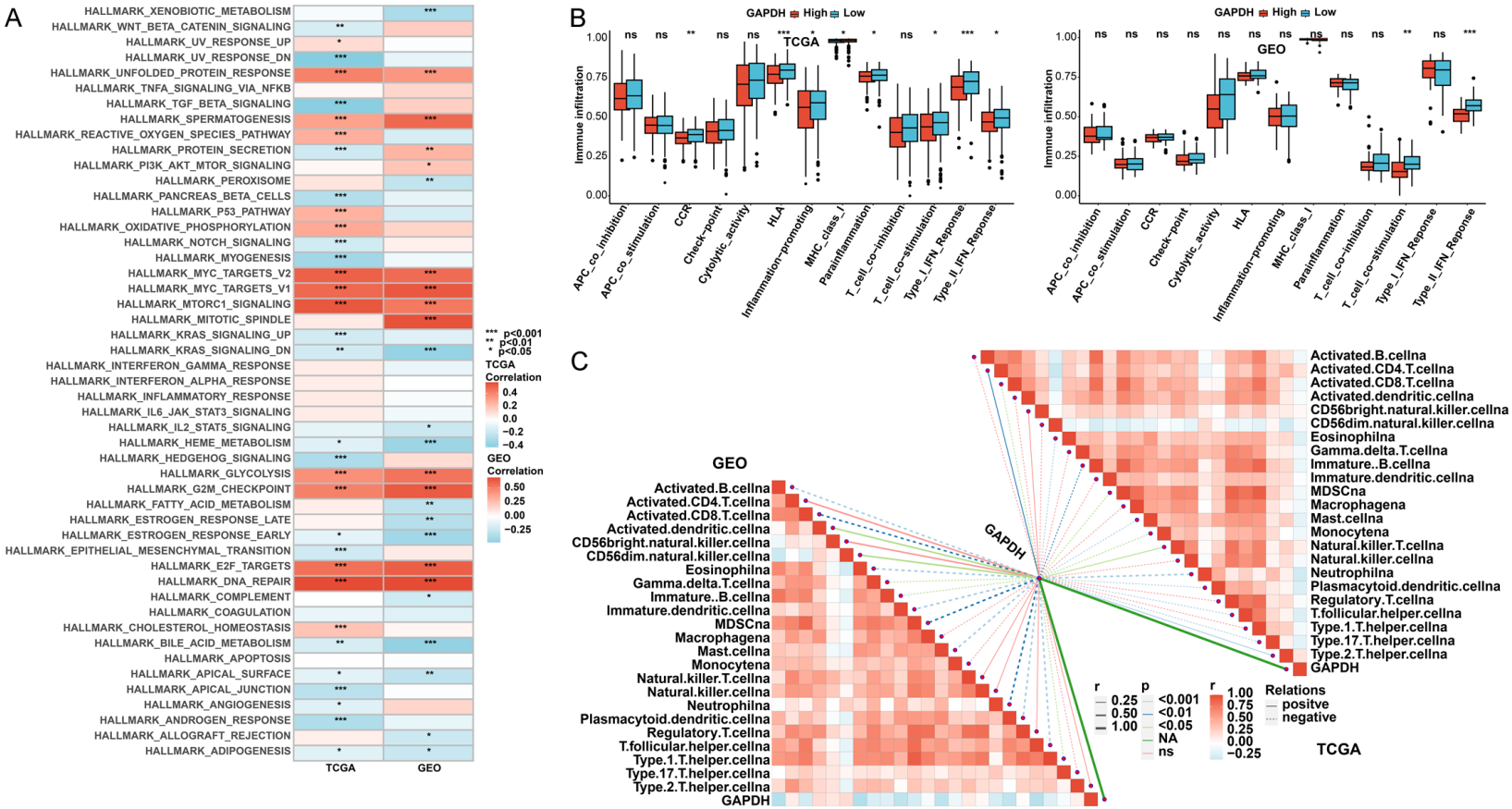


**Figure 7.** Associations of *GAPDH* expression with pathway activation and immune functions in HNSCC. (A, B) Comparative analysis of pathway activation (A) and immune-related functions (B) in HNSCC with high- and low-*GAPDH* expression in TCGA (left or top) and GSE41613 (right or bottom). (C) Spearman correlation analysis displays varying immune cell infiltration abundance significantly associated with *GAPDH* in TCGA (right) and GSE41613 (left). Note: ns, $P>0.05$, ***$P<0.001$, **$P<0.01$, *$P<0.05$.

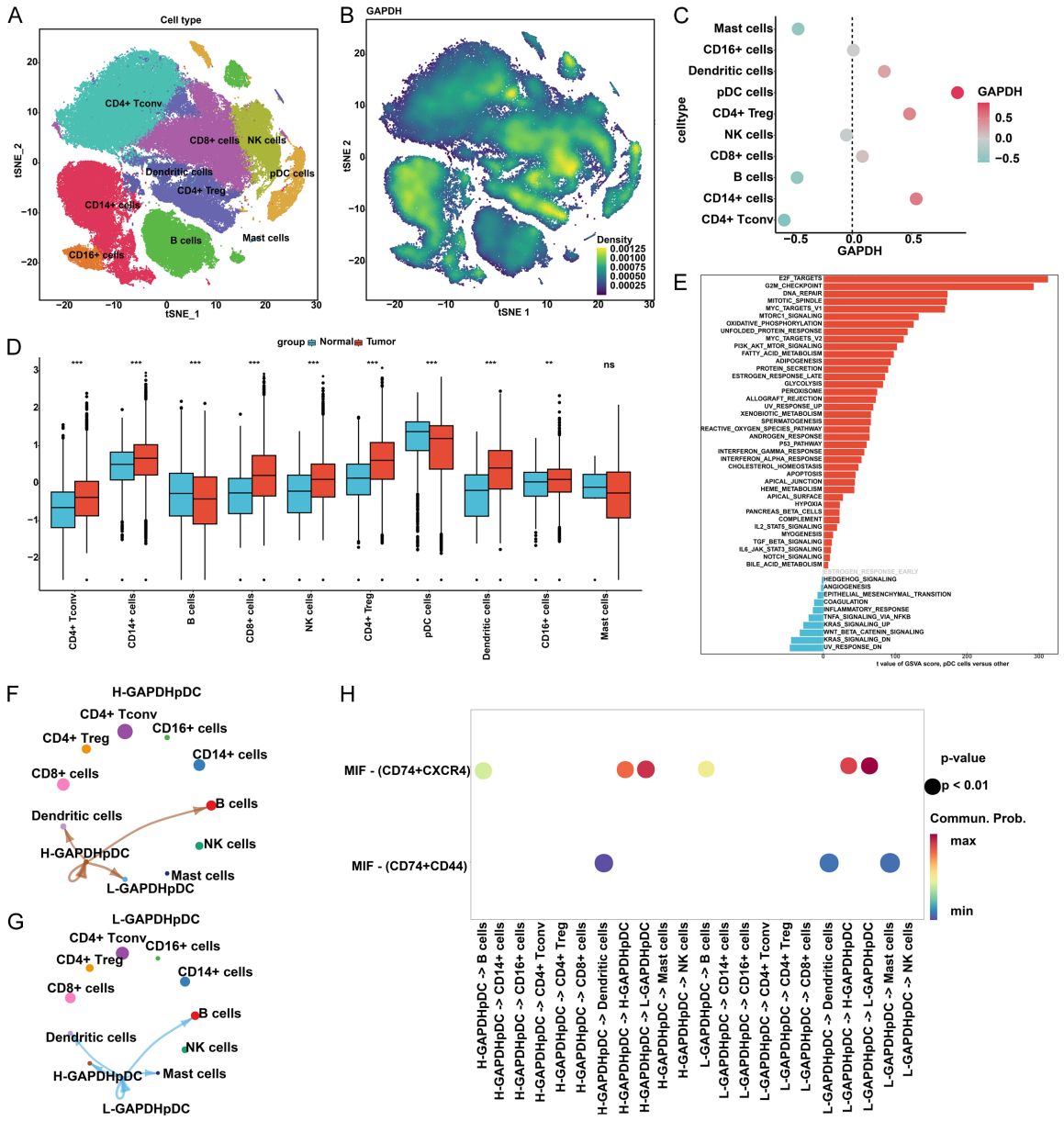


**Figure 8.** Characterization of immune cell subtypes in HNSCC based on *GAPDH* expression using single-cell RNA sequencing analysis. (A) ScRNA-seq data analysis results show annotation of ten subtypes of immune cells in GSE139324 based on the expression of their marker genes. (B) t-SNE plot illustrating the distribution of the ten immune cell subtypes based on *GAPDH* expression. (C) Dot plot depicting the expression levels of *GAPDH* in the ten immune cell subtypes. (D) Comparison of the *GAPDH* expression levels in the ten immune cell subtypes between the HNSCC and normal tissues. (E) GSVA of plasmacytoid dendritic cells (pDC) shows the activation of hypoxia-related pathways in HNSCC. (F, G) Ligand-receptor interactions between high- (F) or low-*GAPDH* expression pDCs (G) and other cell subpopulations. (H) Comparison of the significant ligand-receptor pairs between high- and low-*GAPDH* expression pDC cell subtypes and other cell subpopulations. Note: GSVA, Gene set variation analysis; pDC, plasmacytoid dendritic cells. ns, $P>0.05$, ***$P<0.001$, **$P<0.01$.

mast cells via the *CD74/CD44* receptor-ligand pairing and increased interactions with B cells (**Figure 8F-H**). Therefore, the scRNA-seq analysis results underscore the significant role of *GAPDH* in shaping the TIME. Additionally, they provide further evidence linking *GAPDH* with hypoxia in HNSCC.

### *GAPDH acts as a predictive marker for treatment response and drug resistance in HNSCC*

Immunotherapy and anti-tumor drugs are primary treatments for HNSCC. To discern the potential role of *GAPDH* in prognosticating the clinical response in HNSCC, we investigated

the correlation between *GAPDH* expression and sensitivity to immunotherapy and various drugs. Utilizing data from the TCGA and GEO databases, the TIDE algorithm revealed that, compared to the high *GAPDH* expression group, the low *GAPDH* expression group had a heightened dysfunction score, but a diminished exclusion score ($P<0.05$) (**Figure 9A**). TCIA analyses showed significant differences in the four different immunotherapy response scores between the high *GAPDH* and low *GAPDH* expression groups (all $P<0.05$) (**Figure 9B**). Furthermore, intersectional analyses identified 11 drugs, within the TCGA and GEO datasets, that displayed differential median IC50 values between the high and low *GAPDH* expression groups (**Figure 9C**). Notably, cisplatin, a standard chemotherapeutic agent for HNSCC, exhibited heightened sensitivity in the low *GAPDH* expression group (**Figure 9D**). Similar trends were observed with other drugs, such as Epothilone B (**Figure 9E**, **9F**). Previous studies have reported that increased levels of hypoxia contribute to resistance to a plethora of therapeutic agents [42, 43]. Thus, our findings emphasize the crucial role of *GAPDH* in shaping therapeutic outcomes in HNSCC. They also open new avenues for addressing hypoxia-associated drug resistance.

*GAPDH is overexpressed in hypoxia-treated HNSCC cells and plays a significant role in the progression and cisplatin sensitivity of HNSCC cells*

Hypoxic conditions have been known to elevate *GAPDH* expression in various cells and tissues [20-23]. Interestingly, among human organs, skeletal muscles, which might undergo hypoxia during high-intensity anaerobic activities, display the highest *GAPDH* mRNA levels [44]. Based on this evidence, we theorized that the expression of *GAPDH* might undergo changes in HNSCC under hypoxic conditions. To validate this hypothesis and investigate the specific role of *GAPDH* in HNSCC under hypoxic conditions, we conducted detailed *in vitro* experiments using two HNSCC cell lines, FaDu and TU212, under three distinct oxygen concentrations: 1% $O_2$, 5% $O_2$, and 21% $O_2$. Our results indicated a clear pattern in *GAPDH* expression under these concentrations. HNSCC cells in the 1% $O_2$ environment exhibited the highest levels of *GAPDH* mRNA and protein, with a gradual decline observed at higher oxygen concentrations (**Figure 10A**). This varied expression mirrored cellular behaviors like apoptosis, migration rate, clonogenicity, and invasiveness, with the most aggressive behaviors noted under the 1% $O_2$ condition (**Figures 10B**, **11A-C**). Upon *GAPDH* silencing, we noticed changes in cellular behaviors under all oxygen concentrations. Specifically, the 1% $O_2$+si-*GAPDH* group showed reduced viability compared to its counterpart without *GAPDH* silencing. Similar patterns were observed for the 5% $O_2$ and 21% $O_2$ groups (**Figures 10B**, **11A-C**). Exploring the connection between *GAPDH* expression and chemotherapy sensitivity, our HNSCC cells were exposed to a cisplatin gradient (0, 5, 15, and 20 μg/ml). In the FaDu cell line, a pronounced difference in cell viability was evident at the 24-hour mark starting from the 5 μg/ml concentration across the oxygen environments. For the TU212 cell line, this distinction was apparent starting from the 15 μg/ml concentration. Notably, the resilience to cisplatin was most pronounced in the 1% $O_2$ group, decreasing in the 5% $O_2$ and 21% $O_2$ groups (**Figure 11D**). Silencing *GAPDH* further heightened cisplatin sensitivity under all oxygen conditions, emphasizing the therapeutic potential of targeting *GAPDH*. *GAPDH* is a key enzyme in the glycolytic pathway, which is the primary energy source for tumor cells under hypoxic conditions. Furthermore, Chiche et al reported that *GAPDH* increased the malignancy of non-Hodgkin's B-cell lymphoma by inducing *HIF-1α*, a master regulator of the hypoxic response, via *NF-κB* [45]. This aligns with our observations, emphasizing the significant role *GAPDH* plays in HNSCC under hypoxic conditions. In essence, we demonstrated that hypoxic conditions, particularly at 1% $O_2$, robustly augmented *GAPDH* expression in HNSCC cells, intensifying their malignant behaviors and resistance to cisplatin. Silencing *GAPDH* not only mitigated these behaviors but also amplified the cells' sensitivity to the cisplatin. These findings, in line with prior research [27], underscore *GAPDH*'s potential as both a therapeutic target and hypoxia marker in HNSCC.

## Discussion

As altitude increases, oxygen levels decrease, creating a low-oxygen environment typical of high-altitude regions. This hypoxia notably affects patients with various cancers, including

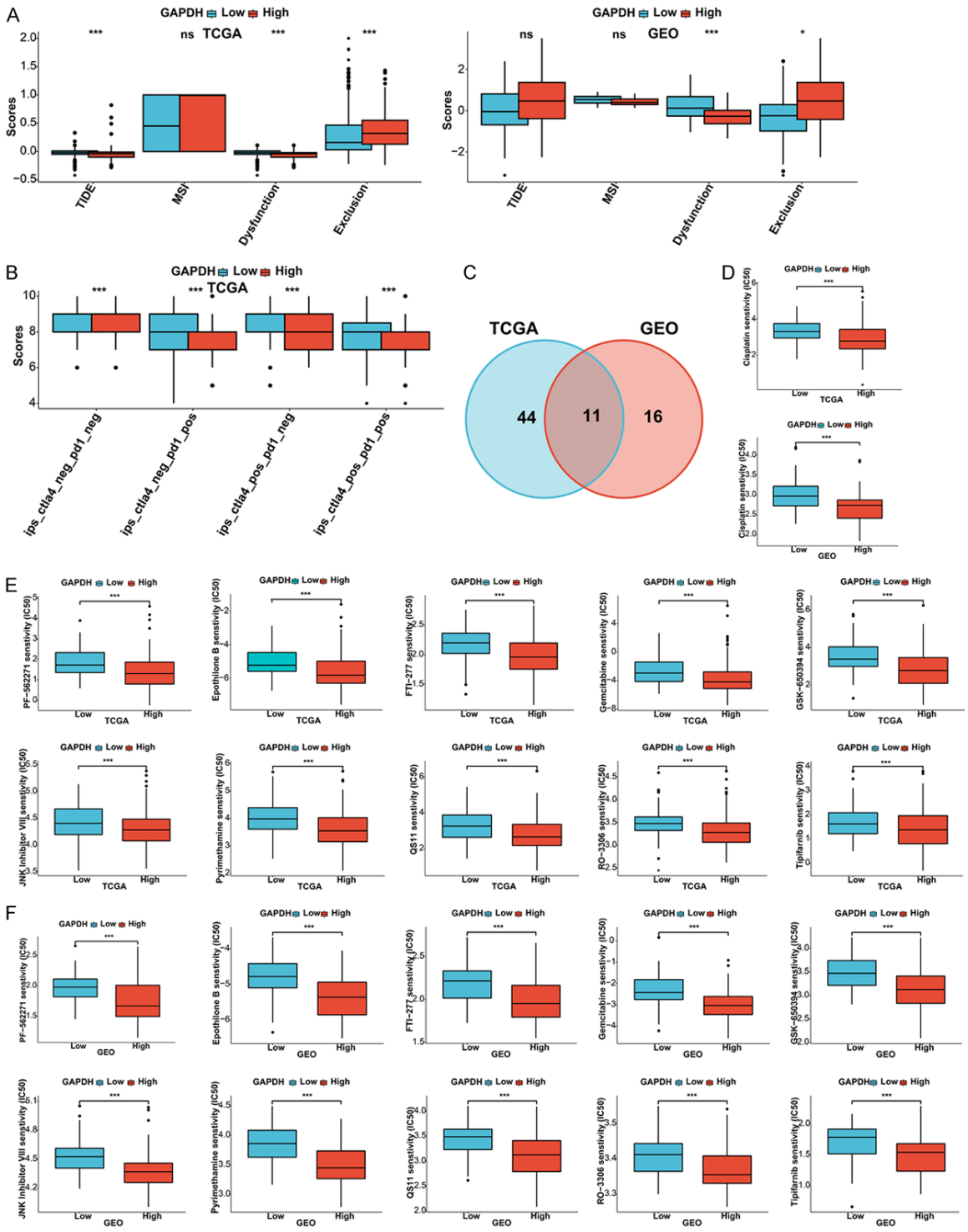


**Figure 9.** Prediction performance of *GAPDH* in determining the efficacy of immunotherapy and anti-tumor drugs in patients with HNSCC. (A) Immunotherapy efficacy outcomes, including dysfunction, exclusion, MSI, and TIDE scores, between high vs. low *GAPDH* expression groups in TCGA (left) and GSE41613 (right). (B) Immunotherapy efficacy scores according to four different scoring methods in the TCIA algorithm for HNSCC patients with high and low *GAPDH* expression levels. (C) The intersections of different sensitive drugs between TCGA and GSE41613. (D) Differences in responses to cisplatin between HNSCC patients in the low vs. high *GAPDH* expression groups from both TCGA (above) and GSE41613 datasets (below). (E, F) Differences in responses to ten drugs between HNSCC patients in the low vs. high *GAPDH* expression groups from both the TCGA (E) and GSE41613 (F) datasets. Note: TCIA, The Cancer Immunome Atlas; MSI, microsatellites; TIDE, Tumor Immune Dysfunction and Exclusion.

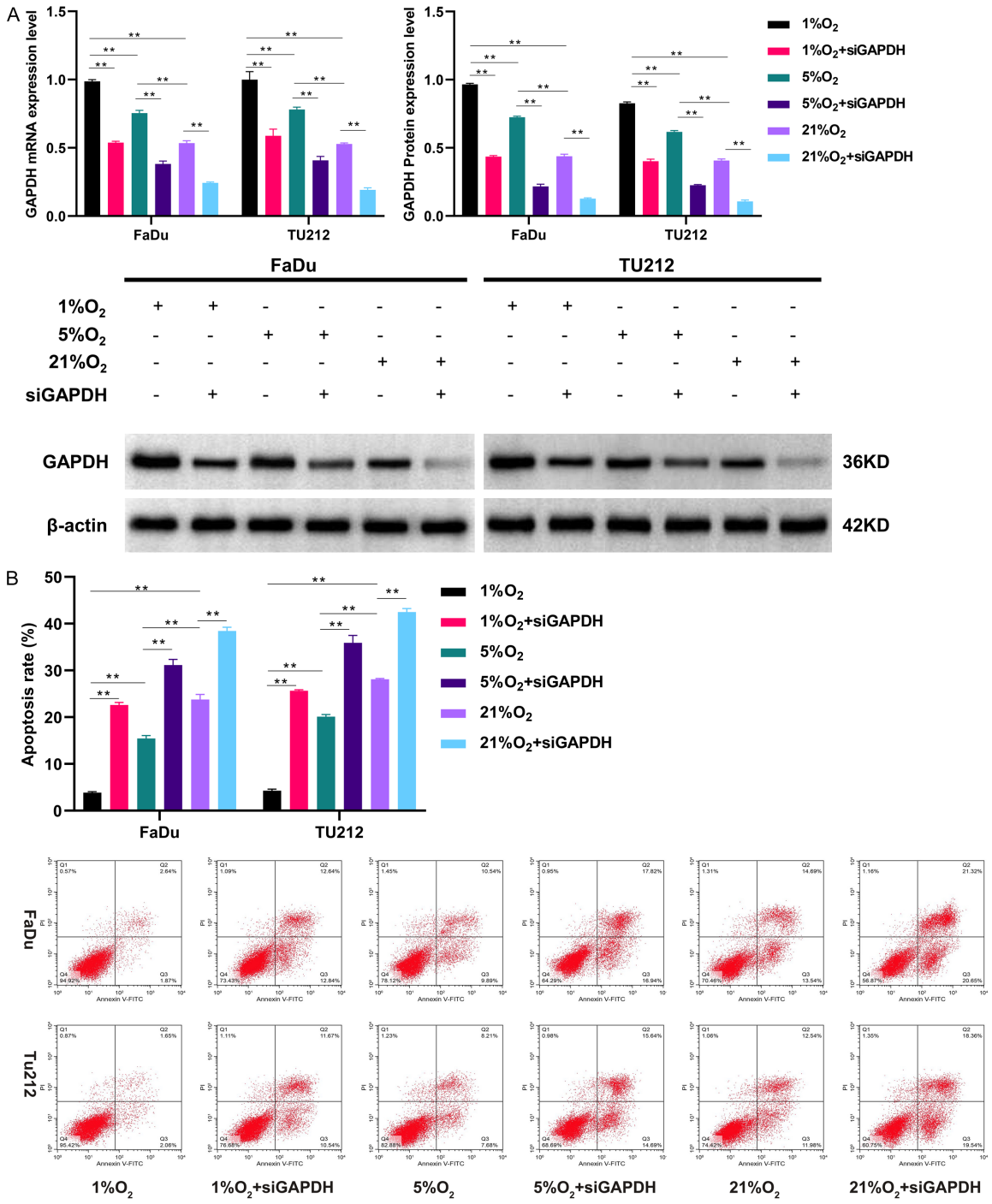


**Figure 10.** Assessing *GAPDH* expression and apoptosis rates in HNSCC cell lines under varying oxygen conditions *in vitro*. (A, B) Evaluation of *GAPDH* mRNA and protein expression levels (A) and apoptosis rate (B) in FaDu and TU212 HNSCC cell lines, exploring distinct oxygen conditions and intervention groups: 1% $O_2$, 5% $O_2$, and 21% $O_2$, as well as si-*GAPDH* transfection followed by exposure to these oxygen levels. Note: ***P*<0.01.

HNSCC. In the saliva of HNSCC patients from these regions, the levels of *miR-122-5p* and *miR-124-3p* diverge significantly from healthy individuals [46]. These miRNAs play a crucial role in hypoxia-driven tumor progression [47, 48]. Inspired by these findings, our study aimed to precisely mimic the hypoxic conditions of high altitudes by examining the effects of dif-

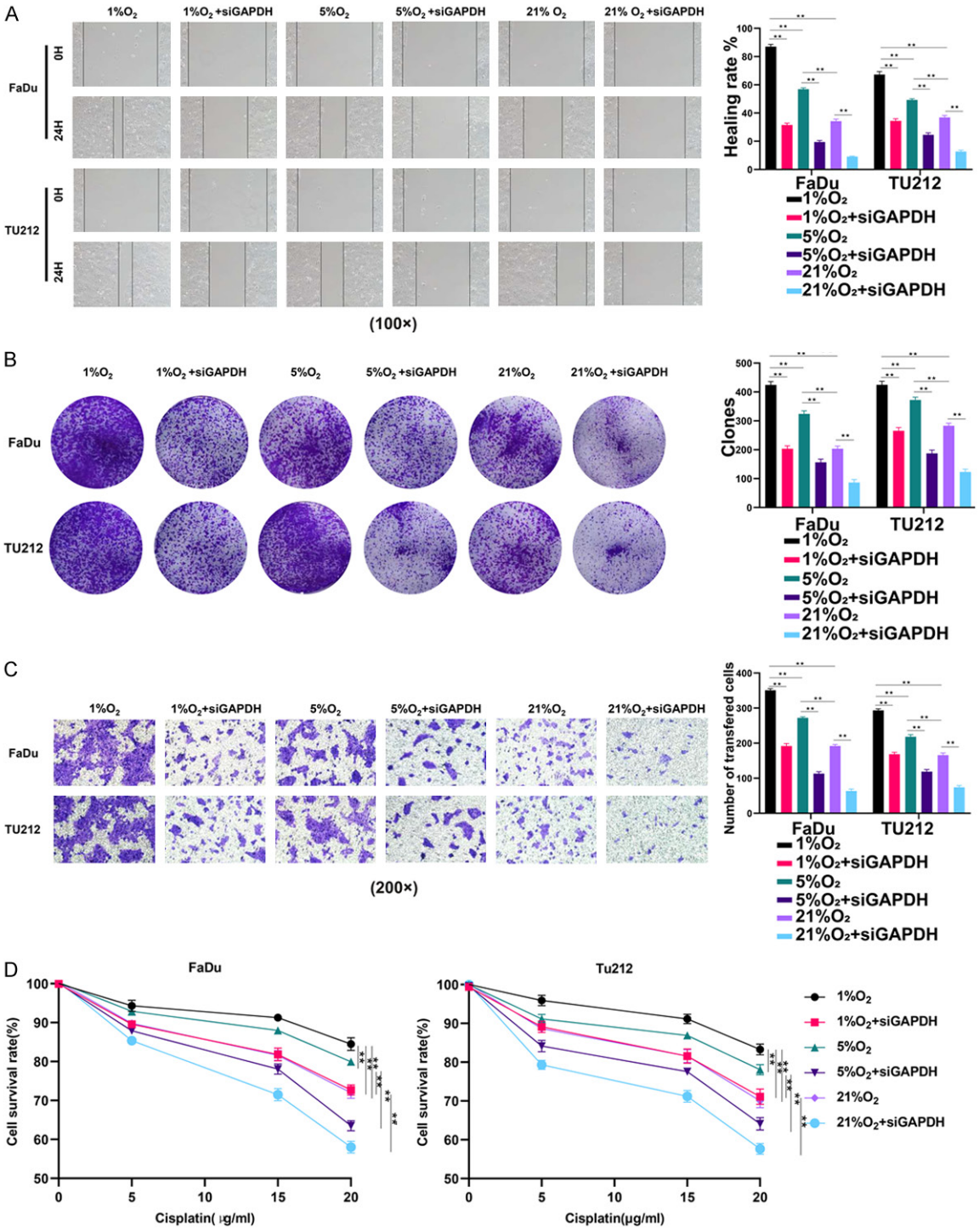


**Figure 11.** Exploring migration, clonogenicity, invasiveness, and viability against cisplatin in HNSCC cell lines under varying oxygen conditions *in vitro*. (A-D) Evaluation of migration (A), clonogenicity (B), invasiveness (C), and viability post-24-hour exposure to various cisplatin concentrations (D) in FaDu and TU212 HNSCC cell lines, exploring distinct oxygen conditions and intervention groups: 1% $O_2$, 5% $O_2$, and 21% $O_2$, as well as si-*GAPDH* transfection followed by exposure to these oxygen levels. Note: ***P*<0.01.

ferent oxygen levels on HNSCC cells. We observed that hypoxia significantly increased HNSCC cell aggressiveness and resistance to cisplatin, especially at a 1% oxygen concentra-

tion compared to 5%. Employing this observational methodology was pivotal, as it unveiled the effects of varying hypoxia levels on cellular behavior, aligning with findings observed in non-small cell lung carcinoma cells [49]. The observed effects are thought to be due to the activation of cancer-promoting factors like *HIF-1α* during hypoxia. Previous research indicates that HIF-1α levels significantly increase under severely reduced oxygen concentrations compared to 5% [50], which might help explain the observed variability in tumors under different hypoxic conditions.

Turning our attention to *GAPDH*, previous studies have notably documented its elevated expression in response to hypoxia across various cells and tissues [20-23], as well as its significant role in managing hypoxic progression in numerous tumors [27, 28]. In our experiments, we observed a notable rise in *GAPDH* expression in HNSCC cell lines under hypoxic conditions, particularly at a 1% oxygen concentration compared to 5%. This elevation might reflect the adaptive responses of cells to the stress of reduced oxygen availability. Importantly, silencing *GAPDH in vitro* not only led to a reduction in HNSCC cell malignancy but also diminished cisplatin resistance. This highlights *GAPDH*'s vital role in hypoxic HNSCC and suggests its potential as a marker for hypoxia severity. Significantly, we also found elevated *GAPDH* levels in advanced-stage tumors, potentially due to their increased malignancy and pronounced hypoxic conditions. This aligns with previous findings of a positive correlation between *HIF-1α* and clinical staging [51]. Furthermore, we observed that patients with higher *GAPDH* expression experienced shorter OS and PFS compared to those with lower expression. This observation affirms the linkage between hypoxia and increased tumor malignancy [52] and aligns with the general observation that patients with pronounced hypoxic features often have worse prognoses [53]. Through our bioinformatics analysis, we uncovered correlations between high *GAPDH* expression and upregulated hypoxia-associated genes, as well as associations with the activation of hypoxia-related and cancer-associated pathways. These insights underscore the pivotal role of *GAPDH* in driving oncogenesis in hypoxic conditions in HNSCC.

Hypoxia enhances both innate and adaptive immune evasion mechanisms, facilitating malignant tumors in evading immune surveillance. Within the context of innate immunity, hypoxia impairs *NK* cell cytotoxicity by attenuating the *STAT3/ERK* signaling pathways through *SHP-1* mediation [54] and hinders dendritic cell maturation and function via *VEGF* signaling [55]. Concerning adaptive immunity, hypoxic conditions lead to reduced activity and cytokine release from various effector cells, including CD4+, CD8+ T cells, and natural killer cells. In contrast, there's an augmentation in the activity and cytokine production of immunosuppressive cells, such as regulatory T cells and M2 macrophages [56]. Altogether, these alterations suggest an immunosuppressive TIME induced by hypoxia. Further research indicates that increased degrees of hypoxia in the TIME are associated with a more pronounced immunosuppressive state [53]. Our analysis revealed differential immune characteristics between groups with high and low *GAPDH* expression. The high *GAPDH* expression cohort exhibited pronounced hypoxia, accompanied by a decrease in infiltrating immune cells. Moreover, inflammatory cells associated with cancer progression, like neutrophil infiltration, positively correlated with *GAPDH* expression, whereas anti-tumor cells, like CD8+ T cells, showed an inverse relationship. The communication between pDC cells with high *GAPDH* expression and other immune cells was diminished, emphasizing the immunosuppressive microenvironment in patients with elevated *GAPDH* levels. Furthermore, we observed increased expression of immune checkpoints, such as *CD276*, in patients with high *GAPDH* expression. Given the known inhibitory roles of immune checkpoints in downregulating immune responses, their activation could impair antitumor immunity [57]. Lastly, the high *GAPDH* expression group demonstrated a higher immunotherapy exclusion score and lower scores in all four TCIA algorithms, hinting at potentially reduced efficacy of immunotherapy in this group, consistent with observed trends in immune infiltration and functionality.

Hypoxia is recognized for its role in enhancing tumor drug resistance, modulating mechanisms such as the *LUCAT1/PTBP1* axis and the *HIF-1α/miR-338-5p/IL-6* feedback loop [58,

59]. Our findings, which reveal lower IC50 scores for 11 drugs in groups exhibiting high *GAPDH* expression, align with previous studies that correlate elevated hypoxia signatures with increased resistance to certain antitumor drugs [11]. These findings are especially intriguing when considering the potential role of hypoxia, indicated by elevated *GAPDH* expression, in modulating drug resistance. The differential responses between *GAPDH* groups might hint at an intrinsic heterogeneity in tumor biology under different hypoxia conditions, which is correlated with drug resistance.

Our study has a few limitations. First, it relied on the comprehensive bioinformatics analyses of data from public databases, which may contain inherent biases. Second, *in vitro* validation using HNSCC cell lines may not fully capture the *in vivo* complexity of the TIME or represent the full spectrum of HNSCC. Third, we identified the association between *GAPDH* and hypoxia in HNSCC, but the specific regulatory mechanism of *GAPDH* in the hypoxic environment of HNSCC remains unclear. Finally, our study was primarily an observational study and did not elucidate the underlying mechanisms that determine the effects of *GAPDH* on tumor progression and treatment resistance. Therefore, further studies employing *in vivo* models and larger patient cohorts, especially those from high-altitude regions, are essential to validate our findings and delve deeper into the molecular mechanisms underlying *GAPDH*'s role in HNSCC.

## Conclusions

Our study demonstrated that elevated *GAPDH* expression in HNSCC is associated with increased malignancy of the tumor, worse survival prognosis, severe hypoxia conditions, and a suppressed immune microenvironment. This augmented *GAPDH* expression also implies resistance to immunotherapies and other antitumor drug treatments. Notably, given *GAPDH*'s pivotal role under varying hypoxic conditions, it emerges as a potential prognostic marker and therapeutic target for HNSCC.

## Acknowledgements

This work was supported by the Guizhou Provincial People's Hospital Hospital-level Youth Fund (Grant No. GZSYQN [2022] 04) and Guizhou Provincial Science and Technology Fund (Qiankehe Foundation - ZK [2021] General 426). The authors would like to express their gratitude to the TCGA and GEO project teams for maintaining the data.

## Disclosure of conflict of interest

None.

**Address correspondence to:** Huiping Ye, Department of Otolaryngology, Guizhou Provincial People's Hospital, Guiyang, Guizhou, China. E-mail: yehuiping888@aliyun.com

## References

[1] Sung H, Ferlay J, Siegel RL, Laversanne M, Soerjomataram I, Jemal A and Bray F. Global cancer statistics 2020: GLOBOCAN estimates of incidence and mortality worldwide for 36 cancers in 185 countries. CA Cancer J Clin 2021; 71: 209-249.

[2] Kim K, Amonkar MM, Hogberg D and Kasteng F. Economic burden of resected squamous cell carcinoma of the head and neck in an incident cohort of patients in the UK. Head Neck Oncol 2011; 3: 47.

[3] Schernberg A, Sagaon-Teyssier L and Schwarzinger M; EPICORL Study Group. Clinical and economic burden of head and neck cancer: a nationwide retrospective cohort study from France. Clinicoecon Outcomes Res 2019; 11: 441-451.

[4] Kase S, Baburin A, Kuddu M and Innos K. Incidence and survival for head and neck cancers in Estonia, 1996-2016: a population-based study. Clin Epidemiol 2021; 13: 149-159.

[5] Marur S and Forastiere AA. Head and neck squamous cell carcinoma: update on epidemiology, diagnosis, and treatment. Mayo Clin Proc 2016; 91: 386-396

[6] Ivan M, Fishel ML, Tudoran OM, Pollok KE, Wu X and Smith PJ. Hypoxia signaling: challenges and opportunities for cancer therapy. Semin Cancer Biol 2022; 85: 185-195.

[7] Bartsch P and Gibbs JS. Effect of altitude on the heart and the lungs. Circulation 2007; 116: 2191-2202.

[8] Chen Q, Duan CB, Huang Y and Liu K. Clinicopathological characteristics and features of molecular subtypes of breast cancer at high altitudes. Front Oncol 2022; 12: 1050481.

[9] Barrera EC, Martinez EZ, Brunaldi MO, Donadi EA, Sankarankutty AK, Kemp R and Dos Santos JS. Influence of high altitude on the expression of HIF-1 and on the prognosis of Ecuador-

ian patients with gastric adenocarcinoma. Oncotarget 2022; 13: 1043-1053.
[10] Garrido DI and Garrido SM. Cancer risk associated with living at high altitude in Ecuadorian population from 2005 to 2014. Clujul Med 2018; 91: 188-196.
[11] Peng C, Ye H, Li Z, Duan X, Yang W and Yi Z. Multi-omics characterization of a scoring system to quantify hypoxia patterns in patients with head and neck squamous cell carcinoma. J Transl Med 2023; 21: 15.
[12] Yun J, Mullarky E, Lu C, Bosch KN, Kavalier A, Rivera K, Roper J, Chio II, Giannopoulou EG, Rago C, Muley A, Asara JM, Paik J, Elemento O, Chen Z, Pappin DJ, Dow LE, Papadopoulos N, Gross SS and Cantley LC. Vitamin C selectively kills KRAS and BRAF mutant colorectal cancer cells by targeting GAPDH. Science 2015; 350: 1391-1396.
[13] Sirover MA. Pleiotropic effects of moonlighting glyceraldehyde-3-phosphate dehydrogenase (GAPDH) in cancer progression, invasiveness, and metastases. Cancer Metastasis Rev 2018; 37: 665-676.
[14] Zhang JY, Zhang F, Hong CQ, Giuliano AE, Cui XJ, Zhou GJ, Zhang GJ and Cui YK. Critical protein GAPDH and its regulatory mechanisms in cancer cells. Cancer Biol Med 2015; 12: 10-22.
[15] Nicholls C, Pinto AR, Li H, Li L, Wang L, Simpson R and Liu JP. Glyceraldehyde-3-phosphate dehydrogenase (GAPDH) induces cancer cell senescence by interacting with telomerase RNA component. Proc Natl Acad Sci U S A 2012; 109: 13308-13313.
[16] Mustafa Rizvi SH, Shao D, Tsukahara Y, Pimentel DR, Weisbrod RM, Hamburg NM, McComb ME, Matsui R and Bachschmid MM. Oxidized GAPDH transfers S-glutathionylation to a nuclear protein Sirtuin-1 leading to apoptosis. Free Radic Biol Med 2021; 174: 73-83.
[17] Yang W, Wang Y, Huang Y, Yu J, Wang T, Li C, Yang L, Zhang P, Shi L, Yin Y, Tao K and Li R. 4-Octyl itaconate inhibits aerobic glycolysis by targeting GAPDH to promote cuproptosis in colorectal cancer. Biomed Pharmacother 2023; 159: 114301.
[18] Peng J, Li W, Tan N, Lai X, Jiang W and Chen G. USP47 stabilizes BACH1 to promote the Warburg effect and non-small cell lung cancer development via stimulating Hk2 and Gapdh transcription. Am J Cancer Res 2022; 12: 91-107.
[19] Guan J, Sun J, Sun F, Lou B, Zhang D, Mashayekhi V, Sadeghi N, Storm G, Mastrobattista E and He Z. Hypoxia-induced tumor cell resistance is overcome by synergistic GAPDH-siRNA and chemotherapy co-delivered by long-circulating and cationic-interior liposomes. Nanoscale 2017; 9: 9190-9201.
[20] Ong HT, Prele CM and Dilley RJ. Using RNA-seq to identify suitable housekeeping genes for hypoxia studies in human adipose-derived stem cells. BMC Mol Cell Biol 2023; 24: 16.
[21] Shayan S, Bahramali G, Arashkia A and Azadmanesh K. In silico identification of hypoxic signature followed by reverse transcription-quantitative PCR validation in cancer cell lines. Iran Biomed J 2023; 27: 23-33.
[22] Kang YM, Shin EJ, Lee BH, Yang JH, Lee HM and Moon SH. Hypoxia regulates the extracellular matrix via mitogen-activated protein kinases pathway in cells retrieved from the human intervertebral disc. Yonsei Med J 2021; 62: 734-742.
[23] Gyongyosi A, Terraneo L, Bianciardi P, Tosaki A, Lekli I and Samaja M. The impact of moderate chronic hypoxia and hyperoxia on the level of apoptotic and autophagic proteins in myocardial tissue. Oxid Med Cell Longev 2018; 2018: 5786742.
[24] Sharma V, Varshney R and Sethy NK. Identification of suitable reference genes for lowlanders exposed to high altitude and ladakhi highlanders. High Alt Med Biol 2022; 23: 319-329.
[25] Xiao J, Li X, Liu J, Fan X, Lei H and Li C. Identification of reference genes in blood before and after entering the plateau for SYBR green RT-qPCR studies. PeerJ 2017; 5: e3726.
[26] Hinkelbein J, Jansen S, Iovino I, Kruse S, Meyer M, Cirillo F, Drinhaus H, Hohn A, Klein C, Robertis E and Beutner D. Thirty minutes of hypobaric hypoxia provokes alterations of immune response, haemostasis, and metabolism proteins in human serum. Int J Mol Sci 2017; 18: 1882.
[27] Gong Y, Zou B, Peng S, Li P, Zhu G, Chen J, Chen J, Liu X, Zhou W, Ding L, Chen Y, Zeng L, Zhang B, Cai C and Li J. Nuclear GAPDH is vital for hypoxia-induced hepatic stellate cell apoptosis and is indicative of aggressive hepatocellular carcinoma behavior. Cancer Manag Res 2019; 11: 4947-4956.
[28] Baptista I, Karakitsou E, Cazier JB, Gunther UL, Marin S and Cascante M. TKTL1 knockdown impairs hypoxia-induced glucose-6-phosphate dehydrogenase and glyceraldehyde-3-phosphate dehydrogenase overexpression. Int J Mol Sci 2022; 23: 3574.
[29] Garcia-Olmo DC, Contreras JD, Picazo MG, Lopez-Torres J and Garcia-Olmo D. Potential clinical significance of perioperative levels of mRNA in plasma from patients with cancer of the larynx or hypopharynx. Head Neck 2017; 39: 647-655.
[30] Liu XS, Zeng J, Zhang YH, Zhang Y, Gao Y, Liu C and Pei ZJ. DARS2 is a prognostic biomarker and correlated with immune infiltrates and cu-

proptosis in lung adenocarcinoma. Am J Cancer Res 2023; 13: 818-834.
[31] Ouyang X, Zhu R, Lin L, Wang X, Zhuang Q and Hu D. GAPDH is a novel ferroptosis-related marker and correlates with immune microenvironment in lung adenocarcinoma. Metabolites 2023; 13: 142.
[32] Fu S, Chen X, Lo HW and Lin J. Combined bazedoxifene and paclitaxel treatments inhibit cell viability, cell migration, colony formation, and tumor growth and induce apoptosis in breast cancer. Cancer Lett 2019; 448: 11-19.
[33] Zhang Y, Cai H, Liao Y, Zhu Y, Wang F and Hou J. Activation of PGK1 under hypoxic conditions promotes glycolysis and increases stem cell-like properties and the epithelial-mesenchymal transition in oral squamous cell carcinoma cells via the AKT signalling pathway. Int J Oncol 2020; 57: 743-755.
[34] Li Q, Shen Z, Wu Z, Shen Y, Deng H, Zhou C and Liu H. High P4HA1 expression is an independent prognostic factor for poor overall survival and recurrent-free survival in head and neck squamous cell carcinoma. J Clin Lab Anal 2020; 34: e23107.
[35] Yang M, Ma B and Liu X. MCTS1 promotes laryngeal squamous cell carcinoma cell growth via enhancing LARP7 stability. Clin Exp Pharmacol Physiol 2022; 49: 652-660.
[36] Zhang G, Zhao X and Liu W. NEDD4L inhibits glycolysis and proliferation of cancer cells in oral squamous cell carcinoma by inducing ENO1 ubiquitination and degradation. Cancer Biol Ther 2022; 23: 243-253.
[37] Kase-Kato I, Asai S, Minemura C, Tsuneizumi K, Oshima S, Koma A, Kasamatsu A, Hanazawa T, Uzawa K and Seki N. Molecular pathogenesis of the coronin family: CORO2A facilitates migration and invasion abilities in oral squamous cell carcinoma. Int J Mol Sci 2021; 22: 12684.
[38] Wong C, Wellman TL and Lounsbury KM. VEGF and HIF-1alpha expression are increased in advanced stages of epithelial ovarian cancer. Gynecol Oncol 2003; 91: 513-517.
[39] Dave B, Granados-Principal S, Zhu R, Benz S, Rabizadeh S, Soon-Shiong P, Yu KD, Shao Z, Li X, Gilcrease M, Lai Z, Chen Y, Huang TH, Shen H, Liu X, Ferrari M, Zhan M, Wong ST, Kumaraswami M, Mittal V, Chen X, Gross SS and Chang JC. Targeting RPL39 and MLF2 reduces tumor initiation and metastasis in breast cancer by inhibiting nitric oxide synthase signaling. Proc Natl Acad Sci U S A 2014; 111: 8838-8843.
[40] Cheng J, Gao F, Chen X, Wu J, Xing C, Lv Z, Xu W, Xie Q, Wu L, Ye S, Xie H, Zheng S and Zhou L. Prohibitin-2 promotes hepatocellular carcinoma malignancy progression in hypoxia based on a label-free quantitative proteomics strategy. Mol Carcinog 2014; 53: 820-832.
[41] Huo Z, Lomora M, Kym U, Palivan C, Holland-Cunz SG and Gros SJ. AQP1 is up-regulated by hypoxia and leads to increased cell water permeability, motility, and migration in neuroblastoma. Front Cell Dev Biol 2021; 9: 605272.
[42] Kopecka J, Salaroglio IC, Perez-Ruiz E, Sarmento-Ribeiro AB, Saponara S, De Las Rivas J and Riganti C. Hypoxia as a driver of resistance to immunotherapy. Drug Resist Updat 2021; 59: 100787.
[43] Fu J, Li T, Yang Y, Jiang L, Wang W, Fu L, Zhu Y and Hao Y. Activatable nanomedicine for overcoming hypoxia-induced resistance to chemotherapy and inhibiting tumor growth by inducing collaborative apoptosis and ferroptosis in solid tumors. Biomaterials 2021; 268: 120537.
[44] Barber RD, Harmer DW, Coleman RA and Clark BJ. GAPDH as a housekeeping gene: analysis of GAPDH mRNA expression in a panel of 72 human tissues. Physiol Genomics 2005; 21: 389-395.
[45] Chiche J, Pommier S, Beneteau M, Mondragon L, Meynet O, Zunino B, Mouchotte A, Verhoeyen E, Guyot M, Pages G, Mounier N, Imbert V, Colosetti P, Goncalves D, Marchetti S, Briere J, Carles M, Thieblemont C and Ricci JE. GAPDH enhances the aggressiveness and the vascularization of non-Hodgkin's B lymphomas via NF-kappaB-dependent induction of HIF-1alpha. Leukemia 2015; 29: 1163-1176.
[46] Salazar-Ruales C, Arguello JV, Lopez-Cortes A, Cabrera-Andrade A, Garcia-Cardenas JM, Guevara-Ramirez P, Peralta P, Leone PE and Paz-Y-Miño C. Salivary microRNAs for early detection of head and neck squamous cell carcinoma: a case-control study in the high altitude mestizo ecuadorian population. Biomed Res Int 2018; 2018: 9792730.
[47] Yang X, Yao B, Niu Y, Chen T, Mo H, Wang L, Guo C and Yao D. Hypoxia-induced lncRNA EIF3J-AS1 accelerates hepatocellular carcinoma progression via targeting miR-122-5p/CTNND2 axis. Biochem Biophys Res Commun 2019; 518: 239-245.
[48] Wang S, Qi Y, Gao X, Qiu W, Liu Q, Guo X, Qian M, Chen Z, Zhang Z, Wang H, Xu J, Xue H, Guo X, Zhang P, Zhao R and Li G. Hypoxia-induced lncRNA PDIA3P1 promotes mesenchymal transition via sponging of miR-124-3p in glioma. Cell Death Dis 2020; 11: 168.
[49] Wang S, Ma H, Li H, Liu Q, Huang S, Huang L, Luo L, Jiang Y and Wu Z. Alternatively expressed transcripts analysis of non-small cell lung cancer cells under different hypoxic microenvironment. J Oncol 2021; 2021: 5558304.
[50] Soroglu CV, Uslu-Bicak I, Toprak SF, Yavuz AS and Sozer S. Effect of hypoxia on HIF-1alpha and NOS3 expressions in CD34(+) cells of

JAK2V617F-positive myeloproliferative neoplasms. Adv Med Sci 2023; 68: 169-175.
[51] Li DW, Zhou L, Jin B, Xie J and Dong P. Expression and significance of hypoxia-inducible factor-1alpha and survivin in laryngeal carcinoma tissue and cells. Otolaryngol Head Neck Surg 2013; 148: 75-81.
[52] Gammon L and Mackenzie IC. Roles of hypoxia, stem cells and epithelial-mesenchymal transition in the spread and treatment resistance of head and neck cancer. J Oral Pathol Med 2016; 45: 77-82.
[53] Li L, Liu W, Tang H, Wang X, Liu X, Yu Z, Gao Y, Wang X and Wei M. Hypoxia-related prognostic model in bladder urothelial reflects immune cell infiltration. Am J Cancer Res 2021; 11: 5076-5093.
[54] Teng R, Wang Y, Lv N, Zhang D, Williamson RA, Lei L, Chen P, Lei L, Wang B, Fu J, Liu X, He A, O'Dwyer M and Hu J. Hypoxia impairs NK cell cytotoxicity through SHP-1-mediated attenuation of STAT3 and ERK signaling pathways. J Immunol Res 2020; 2020: 4598476.
[55] Han Z, Dong Y, Lu J, Yang F, Zheng Y and Yang H. Role of hypoxia in inhibiting dendritic cells by VEGF signaling in tumor microenvironments: mechanism and application. Am J Cancer Res 2021; 11: 3777-3793.
[56] Multhoff G and Vaupel P. Hypoxia compromises anti-cancer immune responses. Adv Exp Med Biol 2020; 1232: 131-143.
[57] Bagchi S, Yuan R and Engleman EG. Immune checkpoint inhibitors for the treatment of cancer: clinical impact and mechanisms of response and resistance. Annu Rev Pathol 2021; 16: 223-249.
[58] Huan L, Guo T, Wu Y, Xu L, Huang S, Xu Y, Liang L and He X. Hypoxia induced LUCAT1/PTBP1 axis modulates cancer cell viability and chemotherapy response. Mol Cancer 2020; 19: 11.
[59] Xu K, Zhan Y, Yuan Z, Qiu Y, Wang H, Fan G, Wang J, Li W, Cao Y, Shen X, Zhang J, Liang X and Yin P. Hypoxia induces drug resistance in colorectal cancer through the HIF-1alpha/miR-338-5p/IL-6 feedback loop. Mol Ther 2019; 27: 1810-1824.

**Supplementary Table 1.** Clinical characteristics of patients with head and neck squamous carcinoma (HNSCC) in the Cancer Genome Atlas (TCGA) dataset

| Variable | TCGA |
|---|---|
| Age at diagnosis (≤60/>60/NA) | 243/253/4 |
| Gender (Male/Female/NA) | 365/132/3 |
| Grade (G1-G2/G3-G4/NA) | 358/119/23 |
| Stage (I-II/III-IV/NA) | 24/406/70 |
| Lymph2deneckdissection (yes/no/NA) | 405/89/6 |
| Method (Surgery/radiationtherapy/Concurrent Chemotherapy/NA) | 92/35/48/325 |
| Radiationtherapy (yes/no/NA) | 252/138/110 |
| Marginstatus (close/positive/negative/NA) | 48/57/341/54 |
| Alcoholhistoryexposures (yes/no/NA) | 329/168/3 |
| Smokeless (yes/no/NA) | 10/212/278 |

**Supplementary Table 2.** Clinical characteristics of patients with HNSCC in the GSE41613 dataset

| Variable | GSE41613 |
|---|---|
| Age at diagnosis (<60/≥60/NA) | 50/47/0 |
| Gender (Male/Female) | 66/31/0 |
| Grade (G1/G2/G3/G4/NA) | / |
| Stage (I-II/III-IV/NA) | 41/56/0 |
| T (T0/T1/T2/T3/T4/NA) | / |
| M (M0/M1/NA) | / |
| N (N0/N1/N2/N3/NA) | / |
| HPV16 (negative/positive/NA) | 97/0/0 |

**Supplementary Table 3.** Clinical characteristics of patients with HNSCC in the GSE139324 dataset

| Variable | Healthy donor | HNSCC |
|---|---|---|
| Age (<60/≥60) | 3/2 | 13/13 |
| Gender (Male/Female) | 3/2 | 20/6 |
| Stage (I-II/III-IV) | - | 12/14 |
| HPV16 (negative) | - | 18/8 |

**Supplementary Table 4.** Detailed primer sequences

| Gene | Forward | Reverse | Sequences |
|---|---|---|---|
| GAPDH | GGTGAAGGTCGGAGTCAACG | CAAAGTTGTCATGGATGHACC | - |
| β-actin | CCTCGCCTTTGCCGA TCC | GGATCTTCATGAGGTAGTCAGTC | - |
| si-GAPDH | - | - | CGGGAAGCUCACUGGCAUG |
| NC-GAPDH | - | - | UUCUCCGAACGUGUCACGUTT |

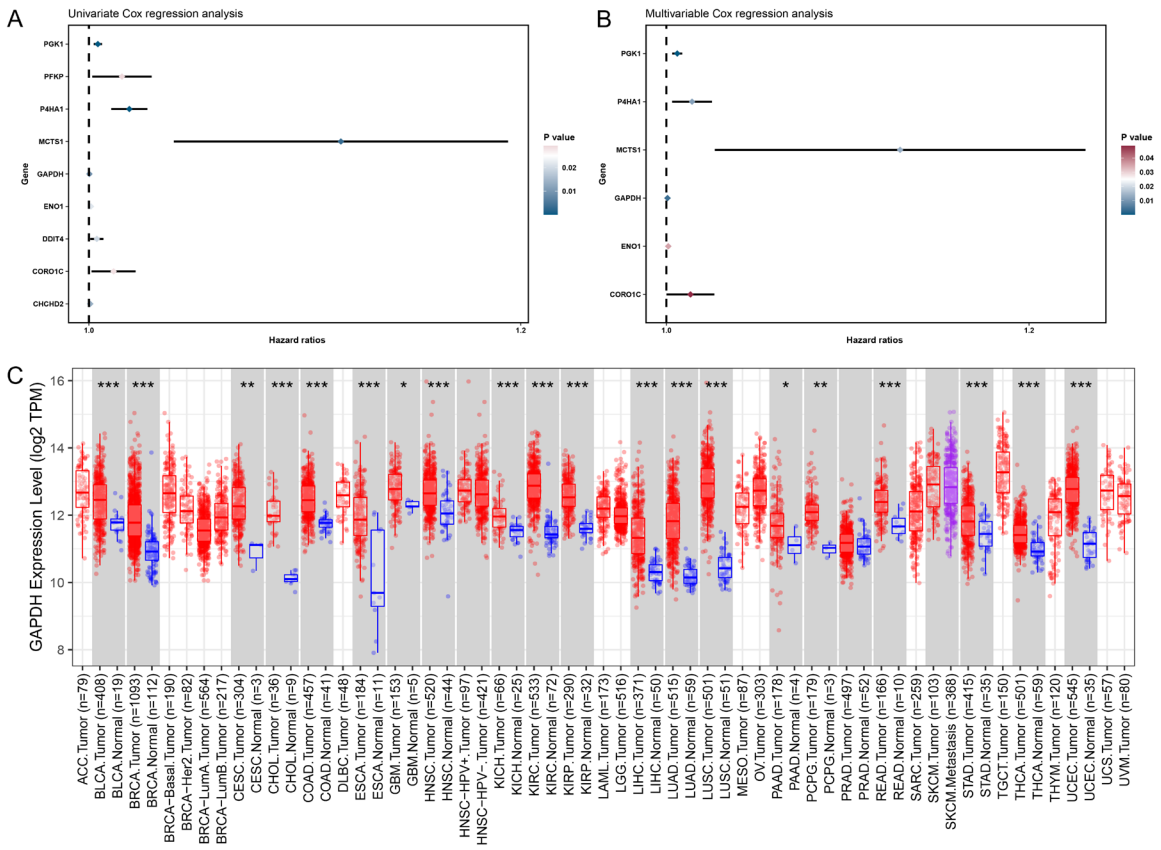


**Supplementary Figure 1.** Univariate and multivariate Cox regression analyses and pan-cancer expression profile of GAPDH. A. Univariate Cox regression analysis of the 49 hypoxia-related genes in HNSCC to determine potential prognostic factors. B. Multivariate Cox regression analysis results for identifying the independent prognostic factors to accurately assess the overall survival (OS) of patients with HNSCC. C. GAPDH expression levels in pan-cancer of TCGA datasets. Note: HNSCC, head and neck squamous cell carcinoma; OS, overall survival. **P*<0.05, ***P*<0.01, ****P*<0.001.